TALLINN UNIVERSITY OF TECHNOLOGY

FACULTY OF CHEMICAL AND MATERIALS TECHNOLOGY
DEPARTMENT OF MATERIALS SCIENCE

TALLINN UNIVERSITY OF TECHNOLOGY SPORTS CENTER BUILDING ROOFTOP GRID-CONNECTED PHOTOVOLTAIC SYSTEM DESIGN

Master Thesis

Semih Hürmeydan

Supervisor: Andres Öpik, Chair of Physical Chemistry,
Professor

Materials and Processes of Sustainable Energetics
2014

Declaration

Hereby I declare that this master thesis, my original investigation and achievement, submitted for the master degree at Tallinn University of Technology has not been submitted for any degree or examination.

....

Name of the student

TALLINNA TEHNIKAÜLIKOOL

KEEMIA- JA MATERJALITEHNOLOOGIA TEADUSKOND
MATERJALITEADUSE INSTITUUT

TALLINNA TEHNIKAÜLIKOOLI SPORDIHOONE KATUSE *ON-GRID* PÄIKESEPANEELIDE SÜSTEEMI TEHNILINE LAHENDUS

Magistritöö

Semih Hürmeydan

Juhendaja: Andres Öpik, füüsikalise keemia õppetool,
Professor

Materjalid ja protsessid jätkusuutlikus energeetikas
2014

Table of Contents

Abbreviations and Acronyms

Air Mass   (AM)

Alternate Current   (AC)

Balance of System   (BoS)

British Thermal Units   (Btu)

Direct Current   (DC)

Internal Rate of Return   (IRR)

Incidence Angle Modifier   (IAM)

Kilowatt hour   (kWh)

Levelized Cost of Energy   (LCOE)

Light Induced Degradation (LID)

Maximum Power Point   (MPP)

Megawatt hour   (MWh)

Meter   (m)

Net Present Value   (NPV)

Nominal Operating Cell Temperature (NOCT)

Photovoltaic   (PV)

Standard Test Conditions   (STC)

Terawatt Hour   (TWh)

1. Introduction

Limited fossil fuels together with the increase in demand for energy all around the world and environmental consequences of conventional energy use provided awareness for renewable energy sources. Therefore, European Union (EU) set a target aiming to get 20% overall share of its energy from renewable sources; 10% share in transport sector and 6% reduction in the greenhouse gas intensity of fuels used in road transport and non-road mobile machinery by 2020 [1]. Estonia, as a member of EU, prioritized an increase in the share of renewable energy.

Compared to the other renewable energy resources, energy production from wind power and bioenergy-based combined heat and power seem to be the prior choices in Estonia since these are the strongest in the country. However, increase in efficiency and reduced manufacturing costs in PV modules during last decade -which is competitive with conventional power production in several countries- presented that electricity production by using PV technology might be cost effective and used as an alternative way to meet demand for electricity at a level of houses and commercial buildings in northern countries.

The objective of this thesis is to design a suiting photovoltaic (PV) system for the roof (flat) of Tallinn University of Technology Sports Center Building. It is expected that the annual energy production from PV systems at this region will be less in comparison with the other countries in the south due to the lower irradiation levels and higher cloudiness in winter seasons.

As a support tool, PVsyst software program is used in this study in order for choosing and sizing PV modules, inverters, calculating shading effects together with the 3D representation, system losses evaluation and simulating different scenarios.

The aim of this study is to bring to a conclusion if there is any way to meet all demand of electricity consumption of Tallinn University of Technology Sports Center Building by using photovoltaic technology and evaluate the best performed design from the point of economics by taking the simple payback period into account.

2. Solar Radiation Geometry

2.1 Solar Radiation

The average power density of solar radiation outside the atmosphere of the Earth is 1367 W/m^2 and this value is named as *solar constant* (G_{sc}). The distance between the Sun and the Earth shows an alteration from 1.47×10^{11} m to 1.52×10^{11} m during a year according to the elliptical orbit geometry of the Earth. For this reason, the solar constant varies in the range of ± 3 % [2].

As shown in Figure 2.1, the distance from the North Pole to the equator on the surface of the Earth is approximately 1×10^7 m and can be used for calculating the radius of the Earth which is known as $(2/\pi) \times 10^7$ m. Therefore, the total power of solar radiation reaching the Earth is:

$$\text{Solar Power} = 1367 \times \frac{4}{\pi} \times 10^{14} \cong 1.74 \times 10^{17} \text{W} \qquad (2.1)$$
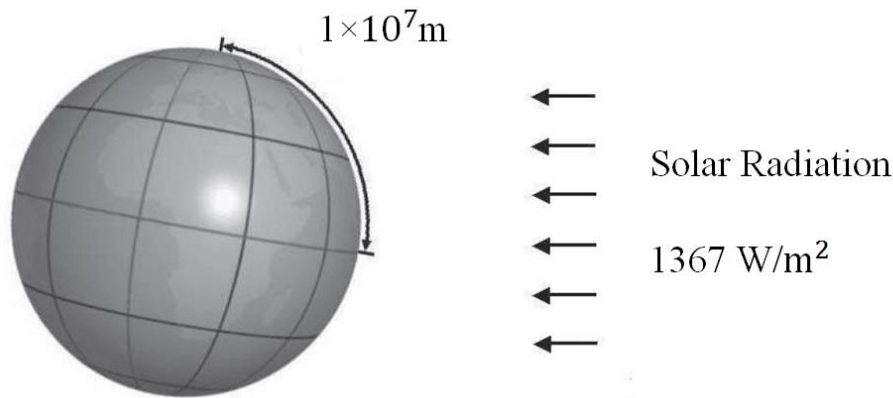
Figure 2.1: Solar constant and length of the meridian from the North Pole to the equator [3].

There are 24 hours in a day and on average, each year has 365.2422 days. The total energy of solar radiation reaching the Earth per year can be calculated by multiplying these values with the total power of solar radiation reaching the Earth (see equation 2.2).

$$\text{Annual solar energy} = 24 \times 365.2422 \times 1.74 \times 10^{17} \cong 15.252 \times 10^{20} \text{ Wh/year}$$

$$= 15.252 \times 10^8 \text{ TWh/year} \qquad (2.2)$$

By taking the solar radiation falling on the atmosphere of the Earth into account, it can be seen that less amount of solar radiation reaches the ground. Approximately, 30% of solar radiation is reflected into space and 20% of solar radiation is absorbed by clouds and molecules in the air. About 75% of the surface of the Earth is water. In brief, the percentage of solar energy absorbed by the ground is around 12.5%. However, even if only 0.01% of total solar radiation is utilizable, it can power the entire world [3].

As seen in Figure 2.2, while annual energy consumption of the entire world was 524 quadrillion British thermal units (Btu) by the year 2010 (equivalent to 15.356×10^4 TWh/year), it is projected that the world's energy consumption will reach up to 819.7 quadrillion Btu by 2040 (equivalent to 24.023×10^4 TWh/year).
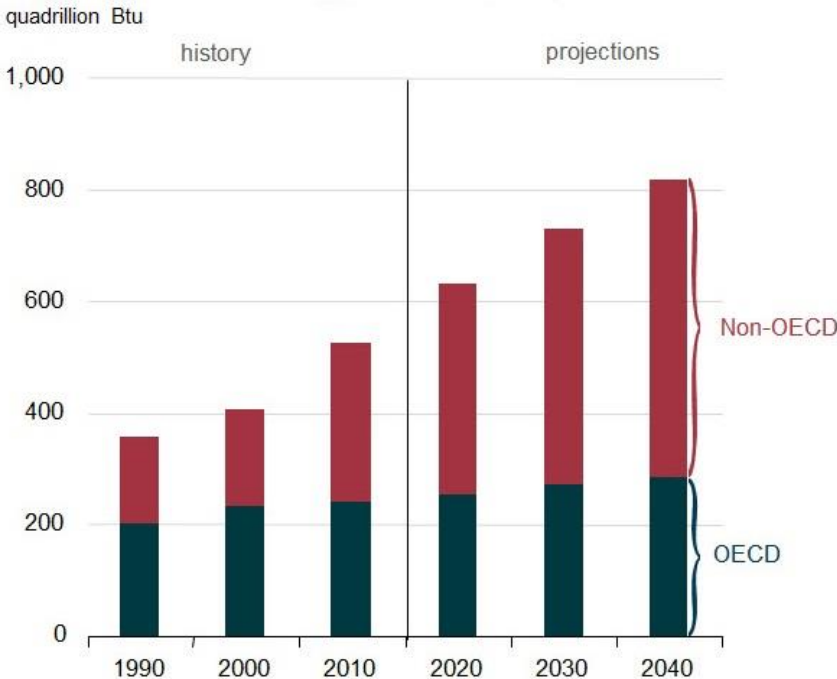
Figure 2.2: World energy consumption, 1990-2040 [4]

2.2 Solar Angles

2.2.1 Solar Declination

The rotation of the Earth around the Sun all the way through a year and around its own axis once a day occur at an angle of 23.45° with respect to the plane of the Earth's direction around the Sun which is named as ecliptic. The axis of the Earth maintains its orientation during a year and this situation leads to the Sun rays coming from changing directions relative to the equatorial plane all year round. This angle between the direction of the Sun rays from the stand point of center of the Sun and the plane of the equator is called solar declination (δ). As illustrated in Figure 2.3, the Earth's axis inclines to the Sun in summer while it has a reverse situation in winter time [5].
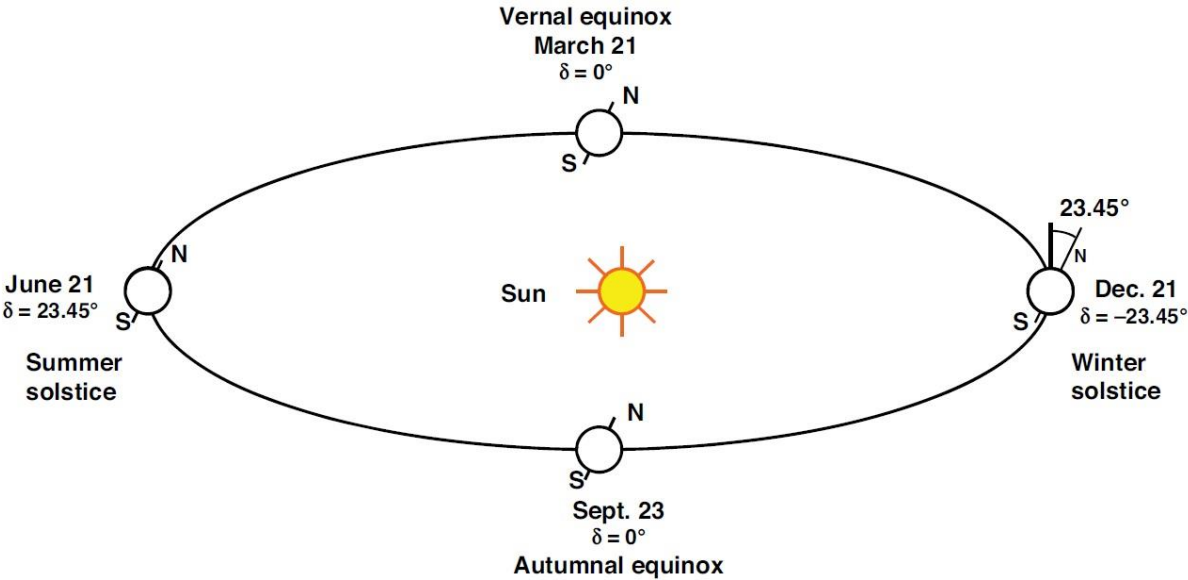
Figure 2.3: The Earth's orbit around the Sun and the position of the Earth's axis over the course of a year [5].

The solar declination varying all the way through the year is shown in Figure 2.4. As seen, the declination angle varies from -23.45° to 23.45° in a year, $-23.45° \leq \delta \leq 23.45°$.

Figure 2.4: Declination of the Sun during a year. [6]

The declination, δ, in degrees can be calculated by using the equation 2.3 for any day of the year [6].

$$\delta = 23.45 \sin\left[\frac{360}{365}(284 + N)\right] \tag{2.3}$$

where N is the number of the days beginning from January 1st.

2.2.2 Solar Altitude and Azimuth

Solar altitude angle (h_s) is defined as the angle between the Sun and horizontal surface, between 0˚ and 90˚; as for solar azimuth angle (γ_s), it is defined as the angular displacement from due south of the projection of the Sun rays on horizontal surface. This angle varies from 0˚ to ± 180˚ (see Figure 2.5).

Figure 2.5: Position of the Sun that is seen from the point P on the Earth via the angles solar altitude (h_s) and solar azimuth (γ_s) [5].

The mathematical expressions for solar altitude and solar azimuth angles are [5]:

$$\sin h_s = \sin \varphi \sin \delta + \cos \varphi \cos \delta \cos \omega \qquad (2.4)$$

$$\sin \gamma_s = \frac{\cos \delta \sin \omega}{\cos h_s} \qquad (2.5)$$

where h_s is solar altitude angle, γ_s is solar azimuth angle, δ is the declination, φ is latitude and ω is the hour angle. Latitude is defined as the angular location north or south of the equator (north positive; $-90° \leq \varphi \leq 90°$) [1]. Hour angle is the difference between noon and the desired time of day in terms of a 360° rotation in 24 hours [7].

At sunrise and sunset, $h_s = 0$. Equation 2.4 yields the following for sunset hour angle (ω_s):

$$\cos \omega_s = - \tan \varphi \tan \delta \qquad (2.6)$$

2.3   Extraterrestrial Solar Radiation

Extraterrestrial radiation (G_{on}) is the intensity (power) of the sun outside the Earth's atmosphere. Solar radiation is the highest outside the Earth's atmosphere on January 3, around 1400 W/m^2; and lowest on July 4th, around 1330 W/m^2. Extraterrestrial radiation outside the atmosphere varying in these values during a year ranges around 3.3% (see Figure 2.6) and it can be calculated for any day of the year (N), starting from January 1st by using equation 2.7.

$$G_{on} = G_{sc} \left[1 + 0.033 \cos(\frac{360N}{365}) \right] \qquad (2.7)$$

where G_{on} is extraterrestrial radiation measured on the plane normal to radiation on the Nth day of the year (W/m^2). G_{sc} is the solar constant (W/m^2) [6].
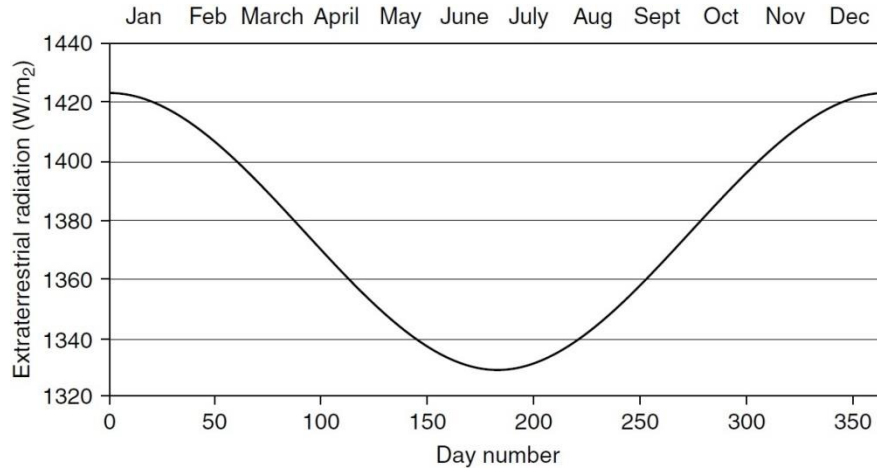
Figure 2.6: Variation of extraterrestrial solar radiation with the time of year [6].

The solar radiation incident on a horizontal plane outside of the Earth's atmosphere which is parallel to the ground is given by the equation 2.8 for a given time of the year.

$$G_{oH} = G_{on} \sin h_s$$

$$= G_{sc} \left[1 + 0.033 \cos(\tfrac{360N}{365}) \right] \left[\sin \varphi \sin \delta + \cos \varphi \cos \delta \cos \omega \right] \qquad (2.8)$$

where G_{oH} is the solar radiation incident on a horizontal plane outside of the Earth's atmosphere, h_s and G_{on} is defined in the equations 2.4 and 2.7 respectively.

The total solar radiation, incident on a horizontal plane during a day can be calculated by integrating equation 2.8 [6].

$$H_o = \frac{24 \times 3600 G_{sc}}{\pi} \left[1 + 0.033 \cos(\tfrac{360N}{365}) \right] \times \left[\cos \varphi \, \cos \delta \sin \omega_s + (\tfrac{\pi \omega_s}{180}) \sin \varphi \, \sin \delta \right]$$

$$(2.9)$$

where H_o is the total solar radiation incident on a horizontal plane during a day, ω_s is sunset hour angle.

14

2.4   The Effect of Atmosphere

When sunlight enters the Earth's atmosphere some is absorbed, some is scattered and some reaches the ground of the Earth without scattering. Sunlight that reaches the Earth's surface without scattering is called direct or beam radiation. Scattered sunlight is called diffuse radiation. Sunlight that is reflected from the ground is called albedo or ground reflected radiation, and the sum of all three components of sunlight is called global radiation [7] (see Figure 2.7).
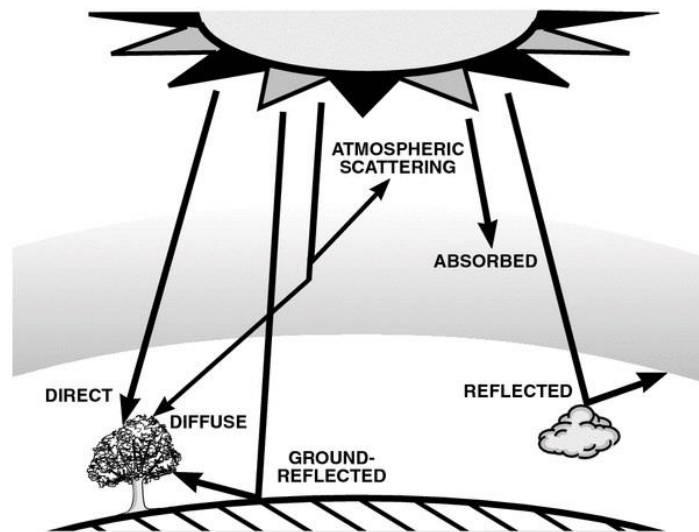
Figure 2.7: The total global radiation on the ground has direct, scattered and reflective components. [8]

The maximum radiation hitting the ground can be observed when the sky is clear and when the Sun is at the top, sunlight has the shortest path length through the atmosphere. This path length is defined as Air Mass (AM). The Air Mass quantifies the reduction in the power of light as it passes through the atmosphere and is absorbed by air and dust. AM is given by the equation 2.10 [9].

$$AM = \frac{1}{\cos \theta_z} \tag{2.10}$$

where θ is the angle from the vertical (zenith angle). When the sun is directly overhead, the Air Mass is 1 (see Figure 2.8).
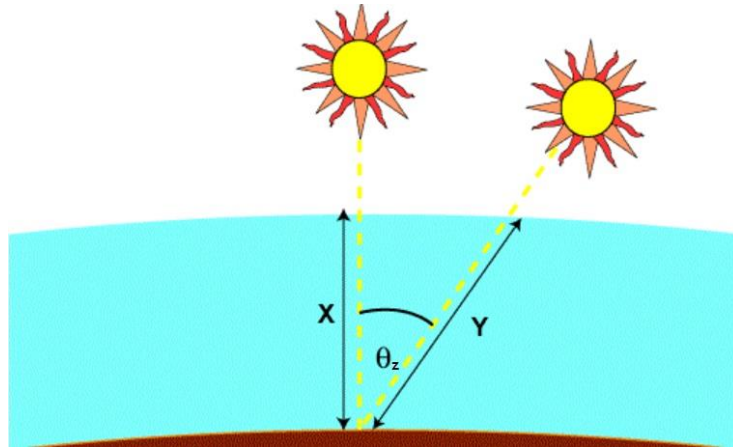
Figure 2.8: The air mass represents the proportion of atmosphere that the light must pass through before striking the Earth relative to its overhead path length, and is equal to Y/X [9].

Figure 2.9 illustrates the correlation between the spectral intensity of solar radiation with regards to the air mass effect in the atmosphere. Reduction in intensity can be seen from the graph depending on the AM0 and AM1.5 values.
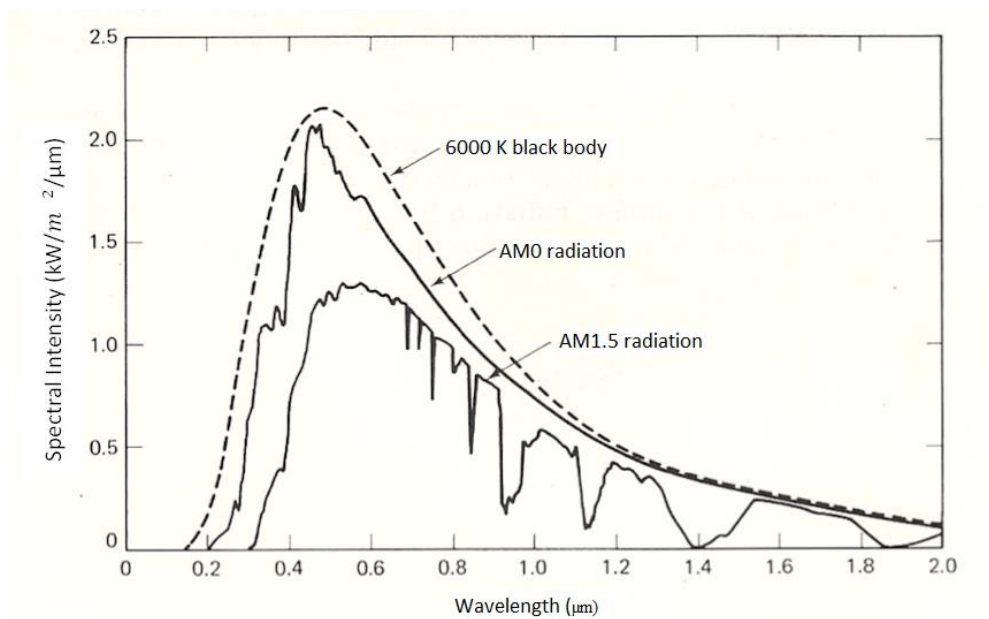
Figure 2.9: Spectral distribution-wavelength graph depending on the air mass [10].

2.5 Hourly Irradiance on an Inclined Surface

Hourly irradiance for any inclined surface (H_t) can be evaluated by using equation 2.11 which is based on a simple isotropic model [11] [12].

$$H_t = H_b R_b + H_d R_d + \rho H R_r \qquad (2.11)$$

where R_b, R_d and R_r are the conversion factors for beam, diffuse and reflected components, respectively; as for ρ, it is known as the reflection coefficient of the ground. H_d and H_b correspond to the diffuse and beam components of H, as for H, it defines the hourly global horizontal irradiance and given by $H = H_b + H_d$.

The radiations outside the atmosphere and on the surface of the Earth are not the same since the atmosphere and clouds reduce the amount. The ratio of the hourly global horizontal irradiance to the corresponding hourly irradiance available outside of the atmosphere is called the hourly clearness index (k_T), and given by [2]:

$$k_T = \frac{H}{H_0} \qquad (2.12)$$

R_b is the ratio of beam radiation on the inclined surface to that on the horizontal surface and given by:

$$R_b = \frac{cos\theta}{cos\theta_z} \qquad (2.13)$$

where θ and θ_z are the incidence angle of beam irradiance on inclined surface and zenith angle of the sun, respectively.

R_d is the ratio of diffuse radiation on the inclined surface to that on the horizontal surface and given by:

$$R_d = \frac{1+cos\beta}{2} \qquad (2.14)$$

where β is the slope of the inclined surface.

R_r is the reflected component from the ground and other surfaces, and is given by:

$$R_r = \frac{1-cos\beta}{2} \qquad (2.15)$$

3.   Grid-Connected Photovoltaic Systems

Grid-Connected Photovoltaic (PV) systems contain PV modules and Balance of System (BoS) components. Main BoS components are:

- Inverters
- Alternating current (AC) and Direct Current (DC) cables
- Mounting Systems
- Disconnect/Isolator Switches
- Junction Boxes
- System Monitoring and Metering

Figure 3.1 gives a simplified schematic diagram of a grid-connected PV system. Some of BoS components are not included in the schema.
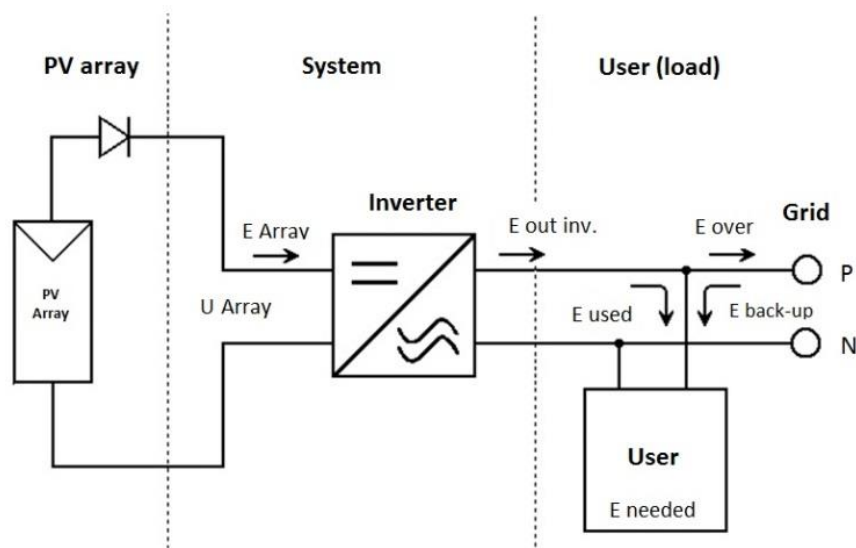
Figure 3.1: Simplified schema of a grid-connected PV system

In this study, only general characteristics of PV modules and inverters are explained.

A basic formation of a PV array; from cell to strings in parallel, can be seen from Figure 3.2. A PV module and a string are the combinations of series connected solar cells and PV modules respectively and the parallel connected strings in a PV array. Figure 3.3, shows a typical PV module with 36 solar cells connected in series.
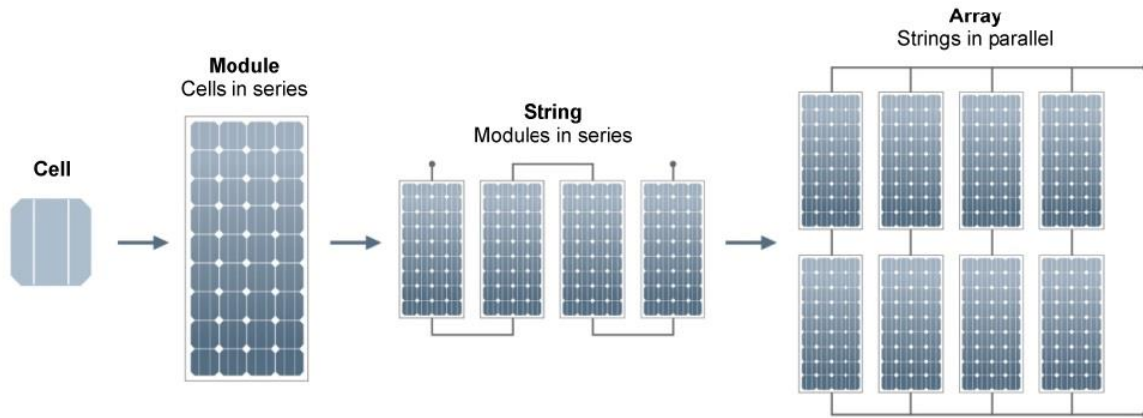
Figure 3.2: Solar cell, PV module, string and array [13].
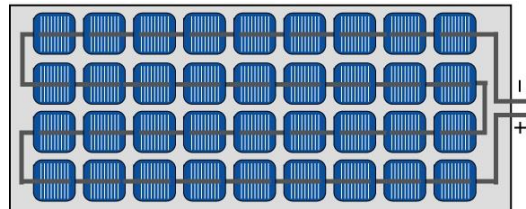
Figure 3.3: Solar cells in series connection [9].

3.1   Solar Cell Characteristics

I-V curve of Figure 3.4 displays of current as a function of voltage of a solar cell at Standard Test Conditions (STC). STC are used with the aim of specifying solar cells and PV modules according to the following values, which are;

Solar Radiation   : $1000W/m^2$

Air Mass (AM)   :   1.5

Cell Temperature   :   25℃
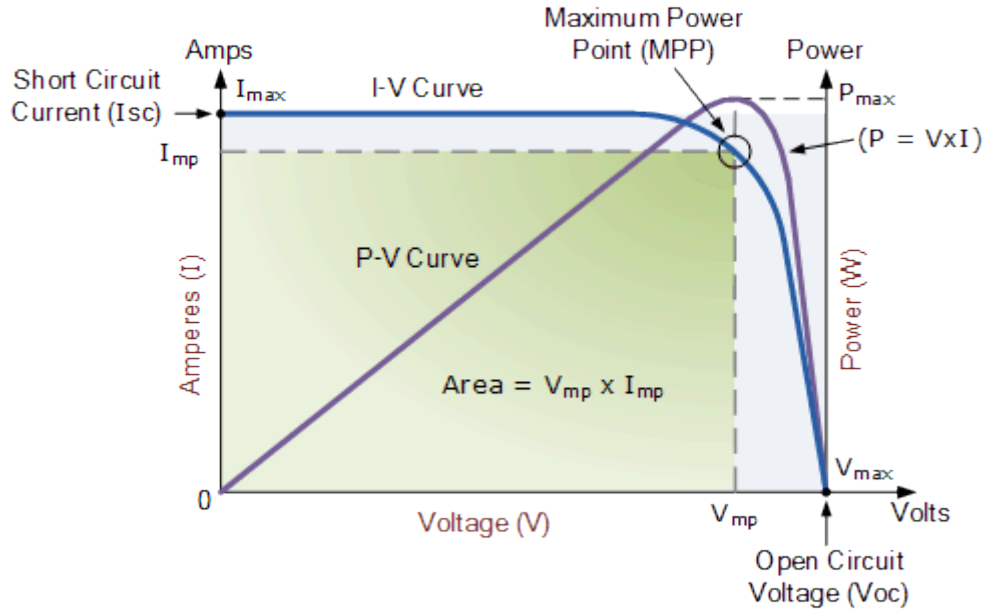
Figure 3.4: I-V and power curves of a solar cell [14].

As seen from the I-V curve of the figure, when the voltage of a solar cell comes to zero point, the current will reach the largest point which is known as short-circuit current and written as I_{SC}. Open-circuit voltage (V_{OC}) is the output voltage of a solar cell when the current is zero at STC. However, neither of these two conditions generates electrical power.

The power curve of the cell represents a correlation between voltage and current ($P = V \times I$) as a product of I-V. In order to achieve maximum output power (P_{max}) under STC at maximum power point (MPP) of I-V curve, the current and voltage values should be determined at the current at MPP (I_{mp}) and the voltage at MPP (V_{mp}). Therefore, It can be said that the ideal operation of a cell occurs at the MPP.

Solar cell efficiency (η_{PV}) is defined as the ratio of P_{max} of solar cell and radiation power arriving at the solar cell (G) (see equation 3.1).

$$\eta_{PV} = \frac{P_{max}}{G \times A_z} \tag{3.1}$$

where A_z is the solar cell area.

Another characteristic definition of a solar cell/module is the fill factor (FF). It is given by equation 3.2 and defined as the ratio of P_{max} to the multiplication of I_{SC} and V_{OC} [5].

$$FF = \frac{P_{max}}{V_{oc} \times I_{sc}}$$

(3.2)

3.2   PV Module/Array Characteristics

A PV module is, in principle, the number cells connected in series with the purpose of increasing power capacity. Efficiency of a solar module (η_M) can be defined as the ratio between module's peak power and the radiation power arriving across the module area. Module efficiency is always lower than the solar cell efficiency (η_{PV}) and given by:

$$\eta_M = \eta_{PV} \times PF$$

(3.3)

where PF is the ratio of total solar cell area to total module area, known as the packing factor of a solar module and always less than 1.

PV modules can be wired in series or in parallel. In many applications, it is possible to see both series and parallel connected PV modules in order to increase the capacity of PV arrays. System voltage and current is determined by the number of PV modules connected in series and parallel, respectively. Figure 3.5 shows the I-V characteristic curves of PV modules according to the connection types. As is seen, the upper right hand corner defines the maximum power point (MPP) of the module and array.
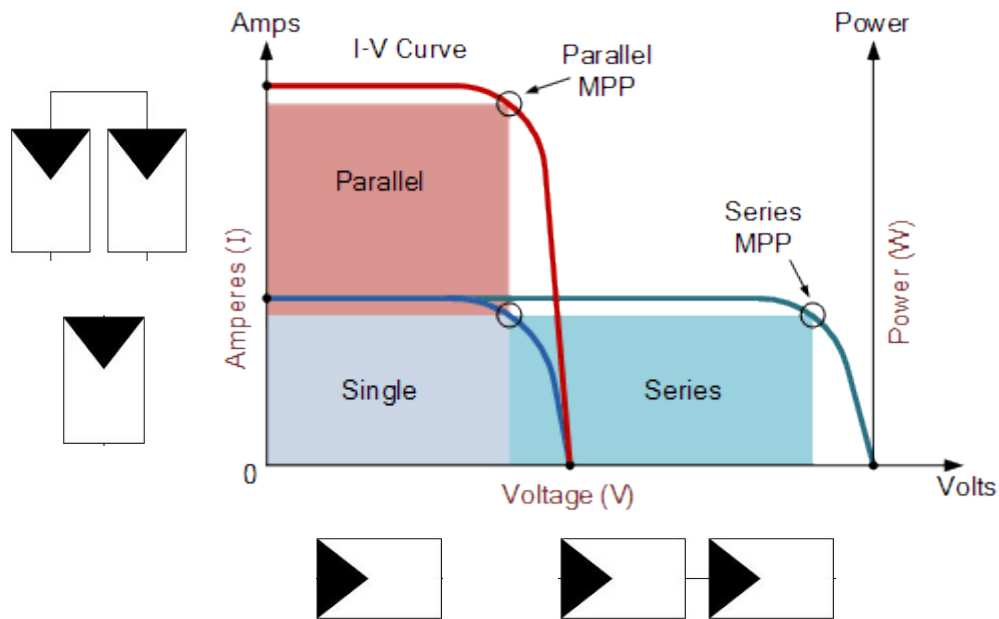
Figure 3.5: Interconnection of PV modules [14].

PV module and array characteristic parameters are affected by varying irradiance level and temperature values. This dependence is illustrated through following graphs (see figure 3.6)

(a)   (b)
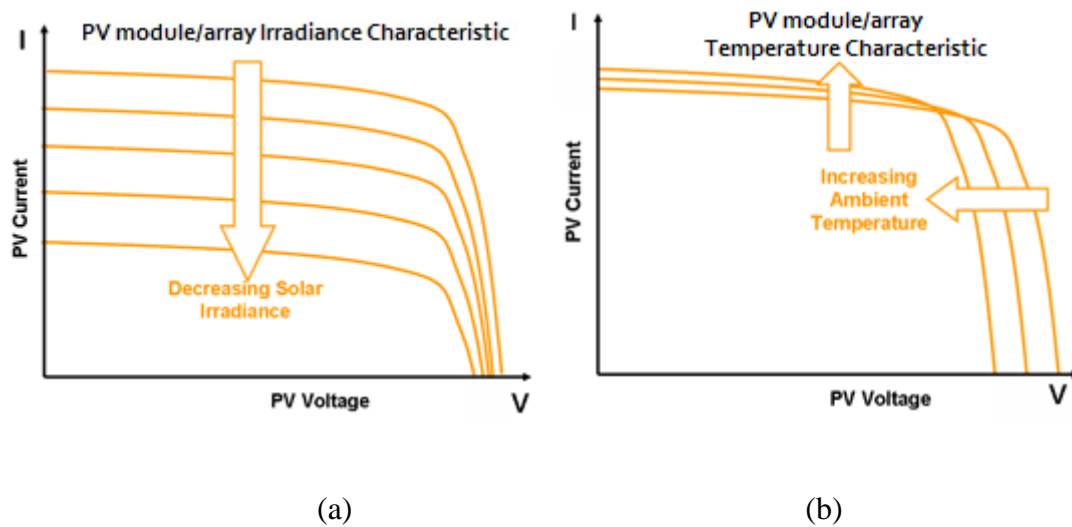
Figure 3.6: PV module/array Irradiance (a), Temperature (b) Characteristics [15].

Figure 3.6 (a) and (b) illustrate the I-V characteristic responses of a module/array with the decreasing irradiance level and increasing ambient temperature, respectively. Decrease in solar irradiance will reduce the current since it is directly related to the number of photons absorbed by the PV modules. On the other hand, an increase in temperature will reduce the

open circuit voltage and increase the current as the resistivity of semiconductors decreases with increasing temperature.

(a)   (b)
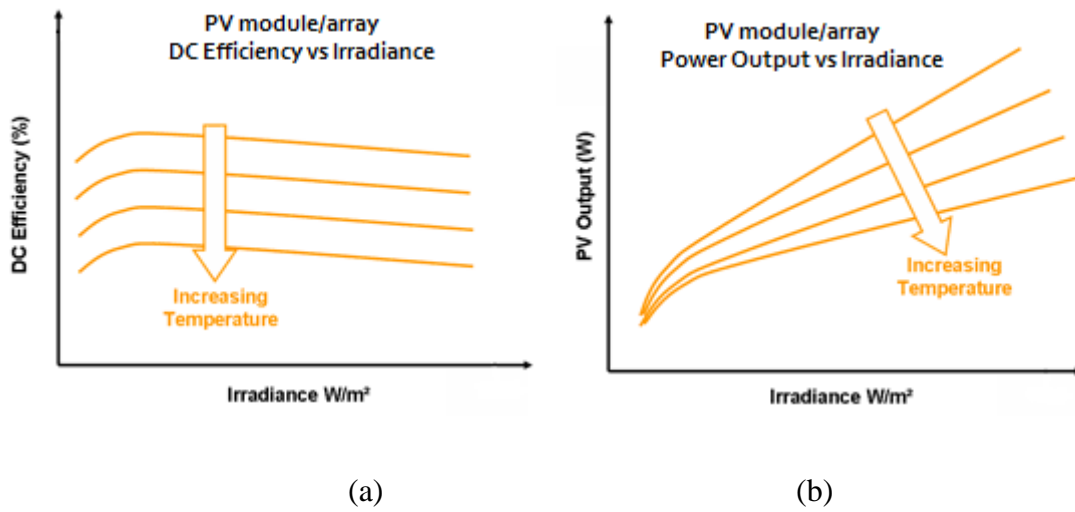
Figure 3.7: PV module/array DC Efficiency-Irradiance (a), Power Output-Irradiance (b) [15].

Figure 3.7 (a) and (b) illustrate the PV module/array efficiency and PV output dependence on irradiance level with increasing temperature. Both the electrical efficiency and the power output of a PV module depend linearly on the operating temperature decreasing with cell temperature [16].

PV modules are rated according to the STC parameters. However, PV modules are generally confronted with lower irradiance level and higher temperature during operations. Therefore, the cell temperature is fixed by Nominal Operating Cell Temperature (NOCT) with respect to the following conditions:

- Irradiance   : $800 W/m^2$
- Ambient Temperature   : $20°C$
- Wind speed   : $1 m/s$

In order to calculate the cell/module temperature for different irradiance and air temperature values, following equation can be used [5].

$$T_m = T_a + \frac{(NOCT-20) \times G_M}{G_{NOCT}} \qquad (3.4)$$

23

where T_m is the module temperature, T_a is the ambient temperature, G_{NOCT} is the NOCT irradiance and G_M is the irradiance on the solar module.

3.3 Inverters

Inverters are used for converting the DC electricity generated by the PV array into AC electricity. Output power can be either single or three phases. According to the total power capacity, size of the inverters may range from hundreds of watts to megawatts [6]. Figure 3.8 shows the circuit diagram symbol of inverters.
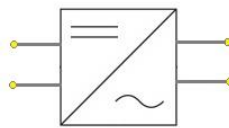
Figure 3.8: Circuit diagram symbol of inverters.

Power output and maximum power point (MPP) of an array show an alteration due to the dependence on irradiance and temperature variance in a daytime. In order to maximize the output power into the grid, inverters track the MPP power which is achieved by the PV array. To do this, inverters move their operating points by adjusting the operating voltage. Tracking and adjusting the MPP point is provided by the MPP trackers in inverters.

As indicated in [17], basic functions of grid-connected inverters can be sorted as;

- *"conversion of the direct current generated by the PV modules into mains-standard alternating current*
- *adjustment of the inverter's operating point to the MPP of the PV modules (MPP tracking)*
- *recording of the operating data and signaling (display, data storage and data transfer)*
- *establishment of DC and AC protective devices (incorrect polarity protection; overvoltage and overload protection; protection and monitoring equipment to keep within relevant national codes and regulations)."*

During conversion from DC to AC power, a power reduction in the inverter will be monitored. This loss which is caused by multiple internal and external factors is represented by the inverter efficiency rates. The power efficiency of an inverter is defined as the ratio of the output power (P_{AC}) and input power (P_{DC}) as given in equation 3.5 [5].

$$\eta_{inv} = \frac{P_{AC}}{P_{DC}} \tag{3.5}$$

However, in order to make comparison between inverters based on their efficiencies under different climatic conditions, it is possible to use weighted efficiency values. Following equation is used for calculating inverter efficiency in European countries what is called Euro efficiency [18].

$$\eta_{EU} = 0.03.\eta_{5\%} + 0.06.\eta_{10\%} + 0.13.\eta_{20\%} + 0.10.\eta_{30\%} + 0.48.\eta_{50\%} + 0.20.\eta_{100\%}$$

$$\tag{3.6}$$

4. Grid-Connected PV System Design in PVsyst

4.1 PVsyst Description

PVsyst is a PC software package for the study, sizing and data analysis of complete PV systems containing grid-connected, stand alone, pumping and DC-grid (public transportation) systems. It provides extensive meteo and PV systems components databases and general solar energy tools. PVsyst is developed at the University of Geneva by Andre Mermoud [19].

Project design in PVsyst is based on the performance analysis through detailed hourly simulations.

The following diagram shows an outline of the project's organization and simulation process (see Figure 4.1).
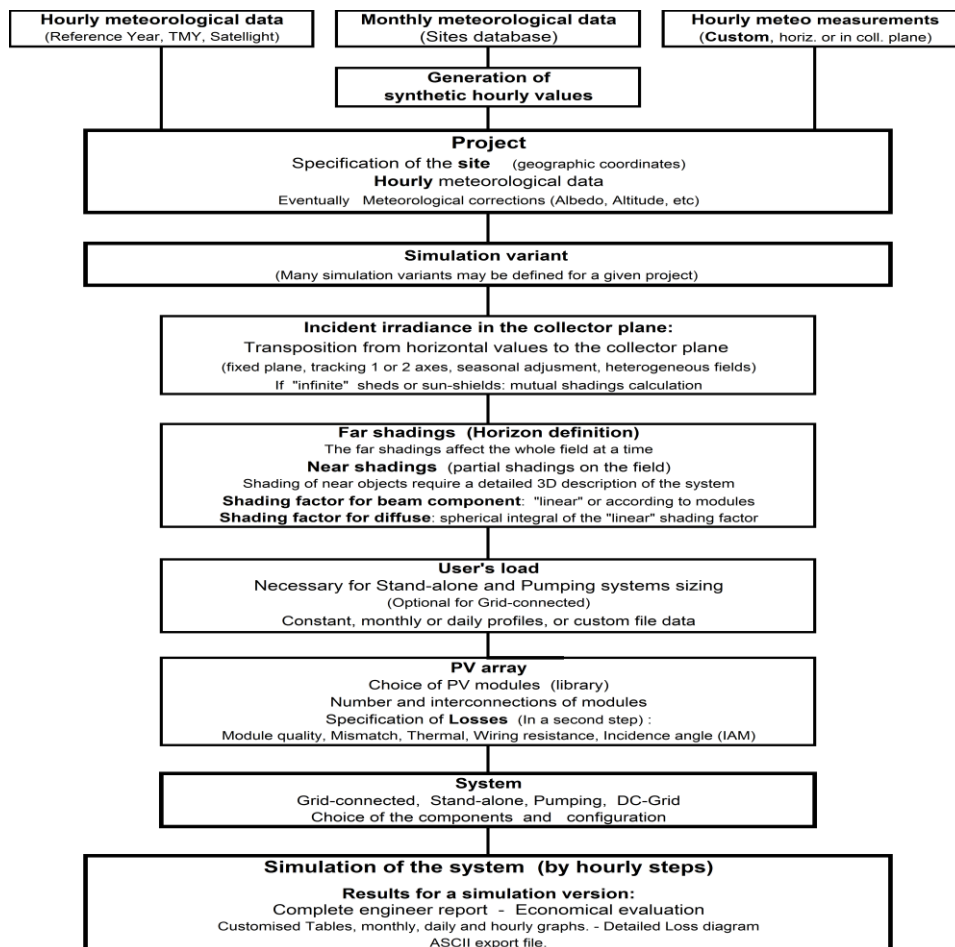
Figure 4.1: Outline of the project's organization and simulation process in PVsyst.

4.2   Site Assessment

It is essential to make a site assessment before designing PV systems to be able to avoid planning errors. This gives a designer an opportunity to see the basic conditions and limiting factors of the site.

The site assessment concerning Tallinn University of Technology (TUT) Sports Center Building rooftop was carried out on the date of April 8th, 2014. Suitability for installation, building orientation and dimensions including height, width and length, available area for installation, far and near shading objects and possible mounting options were investigated during this assessment.

The building is located in Tallinn, Estonia. The geographical coordinates of the site can be seen in Figure 4.2, provided by PVsyst.

Figure 4.2: Project location window in PVsyst.

TUT Sports Center building is fairly in the shape of a rectangular prism so that it is practical to measure the dimensions (see Figure 4.3 (a)) As is seen from Figure 4.3 (b), following numbers were used as measured building parameters in PVsyst; 100m for width, 48m for length, 9m for height and -12° for the azimuth with respect to the south face of the building and 0° for the tilt since the roof is flat.
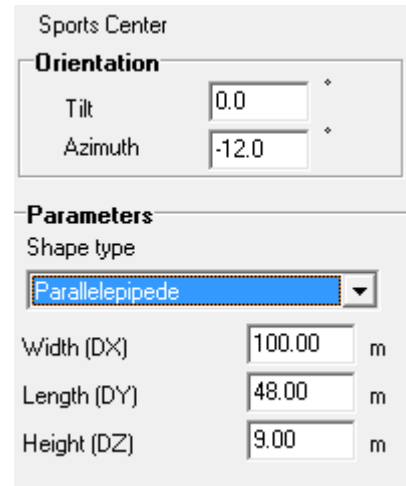
(a)	(b)

Figure 4.3: (a) TUT Sports Center form Google Earth, (b) building orientation and dimensions

Figures 4.4 (a) and (b) show the shading objects on the roof which is certainly taken into consideration during the near shading analysis in PVsyst in order to reduce the loss caused by shading. Figure 4.5 shows a 3D illustration of the building and shading objects on the roof.

(a)	(b)

Figure 4.4: TUT Sports Center Building Rooftop (a) and (b)
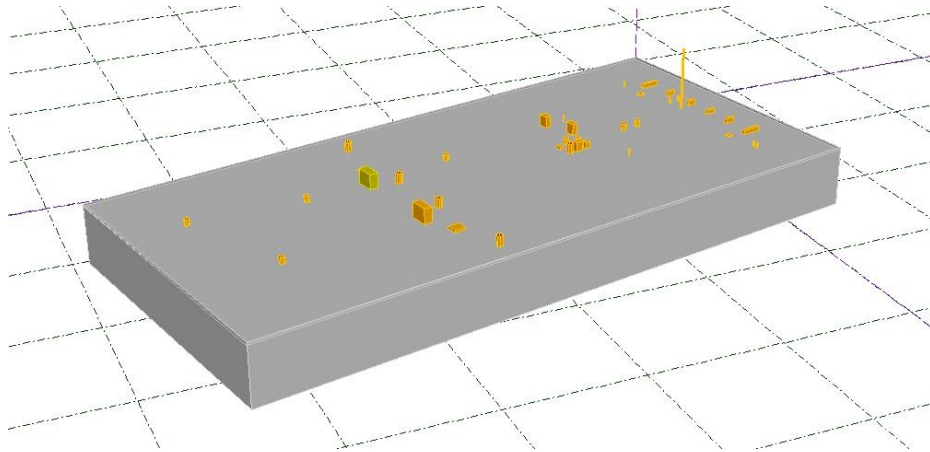
Figure 4.5: 3D representation of the building with shading objects

4.3   Meteorological Data

The accuracy of local meteorological data provided by many sources is highly significant in PV system design processes since this underlies the decision making.

Geographical location data is the first input parameter for generating meteorological data in PVsyst. This gives user a chance to obtain a sun path diagram over the year and to interpolate meteorological data for the locations where no direct measured data is possible to get. Figure 4.6 shows the sun paths at Tallinn and describes the azimuth-sun height correlation according to the specific dates during a year.
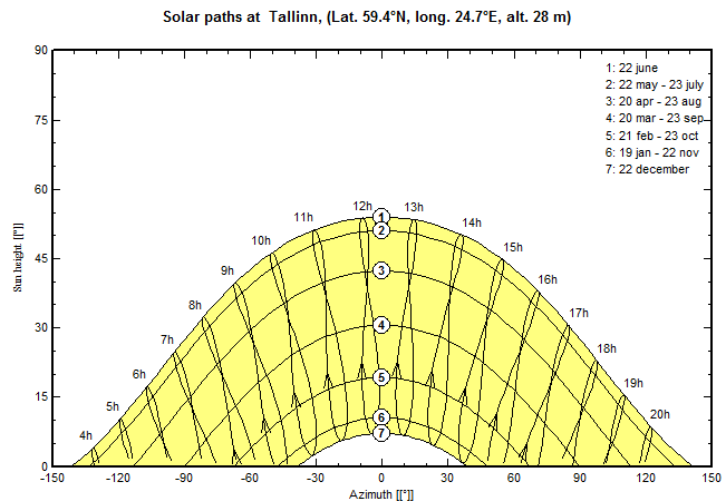
Figure 4.6: Sun path diagram at Tallinn

In PVsyst, the meteorological data used in simulations includes following quantities:

Horizontal global irradiation,

Average External Temperature,

Horizontal diffuse irradiation,

Wind velocity.

Apart from the fact that it is possible to import meteorological data from different databases, the program Meteonorm is used as the main meteorological data sources in PVsyst. As seen, possible sources for importing data into PVsyst are summarized in Table 4.1

| Database	Region	Values	Source	Period	Variables	Availability	PVsyst import
Meteonorm	Worldwide	Hourly	Synthetic generation	1960-1991 and 1995-2000	GHI, DHI, TA VindVel	Included in PVsyst V 6	Direct by site choice
Satellight	Europe	Hourly	Meteosat Any pixel of about 5x7 km²	5 years 1996-2000	GlobH no temper.	Web free	Direct by file
US TMY2/3	USA	Hourly	NREL, 1020 stations Typical Meteo Years	1991-2005 (samples)	GHI, DHI, TA WindVel	Web free	Direct by file
EPW	Canada	Hourly	CWEC, 72 stations Typical Meteo Years	1953-1995 (samples)	GHI, DHI, TA WindVel	Web free	Direct by file
ISM-EMPA	Switzerland	Hourly	22 stations Design Ref. Years	1981-1990 (samples)	GHI, DHI, TA WindVel	Included in PVsyst	Included in database
Solar Anywhere (SUNY model)	USA + Hawaii	Hourly	Satellites by 10x8 km²	1998 - today	GlobH, DiffH Temper for pay Wind for pay	Web 2010 - today for pay	Direct by file
Helioclim - 3 (SoDa)	Europe Africa	Hourly	Meteosat	from 02/2004 => today	GlobH no temper.	Web For pay 2005 free	Direct by copy/paste or PVsyst format
SolarGIS (Geomodel)	Worldwide	Hourly	Meteosat, ERA	1994 - today	GHI, DHI, TA	For pay	Direct (file) PVsyst format
3Tiers	Worldwide	Hourly	Satellites Spectroradiometer MODIS	1998 - today	GHI, DHI DNI available no temper.	For pay	Direct (file) PVsyst format

Table 4.1: Meteorological data sources in PVsyst

PVsyst runs the simulation in hourly steps over a year. In case there is no measured hourly data for the specified location, PVsyst uses special algorithms to generate hourly meteorological data by the way of starting from the monthly data. This is called synthetic data generation. In simulations, generated synthetic hourly data is used for Tallinn city since the monthly meteorological data is the only available option for this location. Figure 4.7 shows the Tallinn city monthly meteorological data used in the simulations.
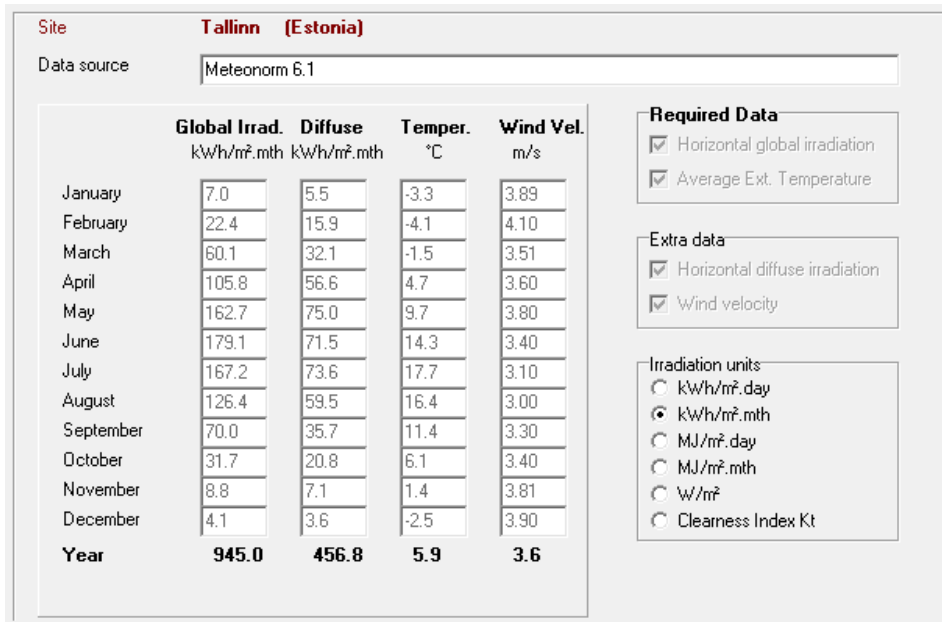
Figure 4.7: Monthly meteorological data used in PVsyst.

"The albedo coefficient is the fraction of global incident irradiation reflected by the ground in front of a tilted plane [20]". The value of 0.2 is set as default in PVsyst and accepted as a standard, however it is possible to change the value according to physical conditions of the project location (see Figure 4.8). It is assumed that the default value is more realistic for the project location and therefore albedo value is taken as 0.2 and used in the simulations.
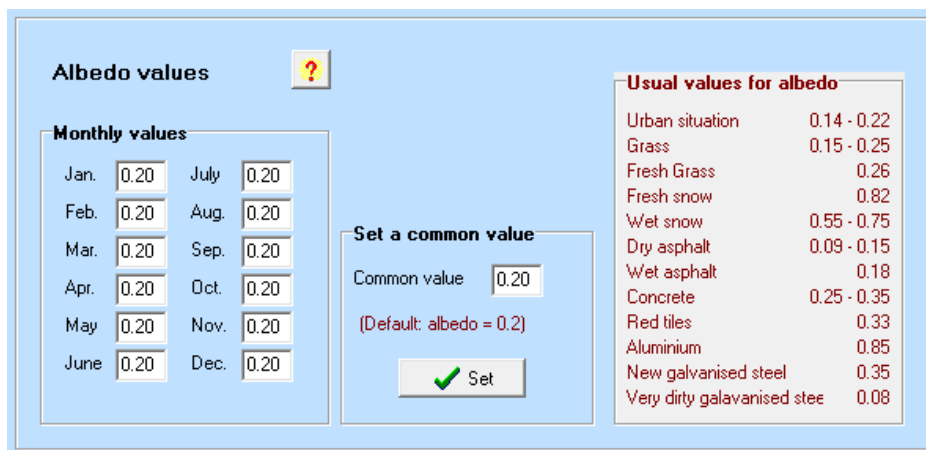
Figure 4.8: Albedo values in PVsyst.

When sizing the PV array voltage according to the inverter specifications, variation in module temperature should be taken into account depending on the air temperature and irradiation on

module. Before starting with the module orientation, PVsyst requires from the user to specify four site-dependent parameters which are defined under *Albedo - Settings* dialog. These are the reference temperatures for the design of the PV array (see Figure 4.9).

Lower temperature for Absolute Voltage limit parameter defines the minimum temperature ever measured at the project location and used to determine the maximum array voltage. -10°C is used as a default value in PVsyst which is mainly practical for Central European countries. However, as the lowest recorded temperature in Tallinn for last 30 years is -32.2°C [21], it is used in simulations as a design parameter.

Usual operating temperature under $1000/m^2$ parameter is not used for sizing constraints, therefore the default value 50°C was not changed.

Winter operating temperature for $V_{MPP}max$ *design* and *summer operating temperature for* $V_{MPP}min$ *design* parameters define the minimum and maximum cell temperatures in operating conditions, respectively. Default values are 20°C and 60°C. However, according to the irradiance and temperature data provided by PVsyst, these parameters were altered to 2°C and 69°C, based on Equation 3.4. For *summer operating temperature for* $V_{MPP}min$ *design* parameter, highest recorded temperature in Tallinn, 34.3°C [21] is used (also see Appendix 3)
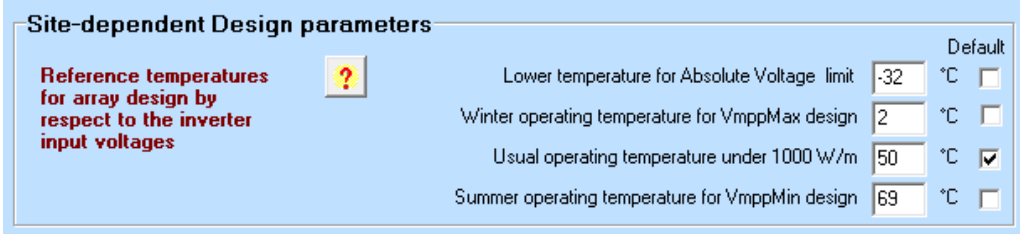
Figure 4.9: Site-dependent design parameters in PVsyst.

4.4 Module Orientation

Optimization of a module orientation is an important process in order to collect as much irradiance as possible on the surface of the module. To be able to this, module tilt angle (β) and azimuth angle (γ$_s$) should be optimized. The module tilt angle is defined as the angle between the plane and the horizontal (see Figure 4.10). The module azimuth is defined as the

angle between south and collector plane for northern hemisphere and taken as negative toward east.
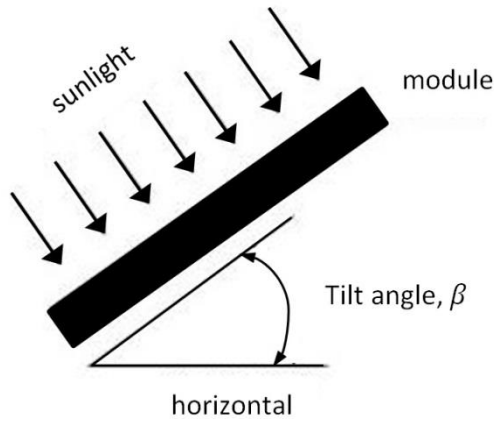
Figure 4.10: Illustration of module tilt angle.

PV modules should be directed towards south ($\gamma_s = 0°$) in northern hemisphere in order to collect maximum available irradiation on the plane.

Optimum tilt angle is determined according to the plane orientation modes, such as fixed tilted plane or seasonal tilt adjustment. In this study only fixed tilted plane orientation is discussed.

The general rule of thumb to determine the optimal tilt angle is taking latitude equal to tilt angle. However, as for the locations with larger latitudes, the difference between winter and summer irradiation increases. Therefore optimal tilt angle differs from the latitude of location. For the purpose of determining the optimal tilt angle according to this locations, following linear equation is accepted as a common approach [22] (see Equation 4.1).

$$\beta_{opt} = 3.7 + 0.69|\varphi| \tag{4.1}$$

Where β_{opt} is the optimum tilt angle and φ is the latitude. When using Equation 4.1 for Tallinn city location, β_{opt} is calculated as 44.6˚. On the other hand, optimized tilt angle in PVsyst is calculated as 39˚ and used in simulations. It is assumed that this differentiation is resulted from local meteorological data in PVsyst that includes cloudy days and its effect on irradiation in Tallinn.

4.5 PVsyst and Orientation

The optimization of module orientation in PVsyst is first done by choosing the field type, then the module orientation mode should be determined in between three options; yearly irradiation yield, summer and winter. The solar panels in this study is installed on a fixed tilted plane and optimized by respect to the yearly irradiation yield. When choosing the fixed plane orientation, an information panel is screened, including transposition factor, the loss with respect to the optimum orientation, and the available irradiation on this tilted plane (see Figure 4.11). The transposition factor is the ratio between irradiation on the plane and horizontal irradiation.
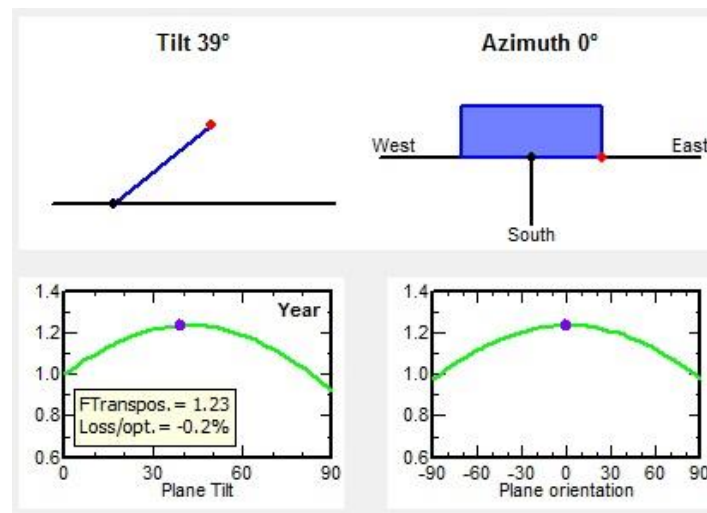
Figure 4.11: Transposition factor as a function of azimuth and plane tilt

The loss by respect to the optimization can be used for determining the optimal tilt angle by changing plane tilt by the time the loss decreases 0%. However, this tool performs quick transpositions from monthly-meteo values and gives a quick estimation which may differ from the hourly meteorological values. To be able to avoid this situation, hourly incident irradiation values on different azimuth and tilted planes were used to determine the optimal tilt angle which is possible to provide from PVsyst. Table 4.2 shows the total global incident in collector plane (Wh/m^2) during a year with respect to different tilt angles. As is seen, 39° gave the highest value and therefore, it is used in the simulations.

Azimuth(°) Tilt (°)	0
35	1118600
36	1119453
37	1120008
38	1120307
39	1120379
40	1120145
41	1119666
42	1118930
43	1117964
44	1116713
45	1115227

Table 4.2: Total yearly irradiation (Wh/m^2) at Tallinn according to the azimuth and tilt angles.

4.6   Inter-Row Spacing

The row of modules in front causes self-shading those on the back row as part of rack-mounting systems. "*Space requirements and shading losses can be minimized through optimization of the tilt angles and distances between the module rows [17].*" After optimizing the orientation of PV modules, inter-row spacing should be arranged according to module width, module tilt angle and position of the Sun. Equation 4.2 is used for calculating the shadow length of a module, the same for the distance [23].

$$\text{D} = \left[(\text{W}\cos\beta) + \left(\frac{\text{W}\sin\beta\cos\gamma_s}{\tan h_s} \right) \right] \tag{4.2}$$

where W is width of modules, β is module tilt angle, γ_s and h_s are solar azimuth and altitude angles respectively (see Figure 4.12).
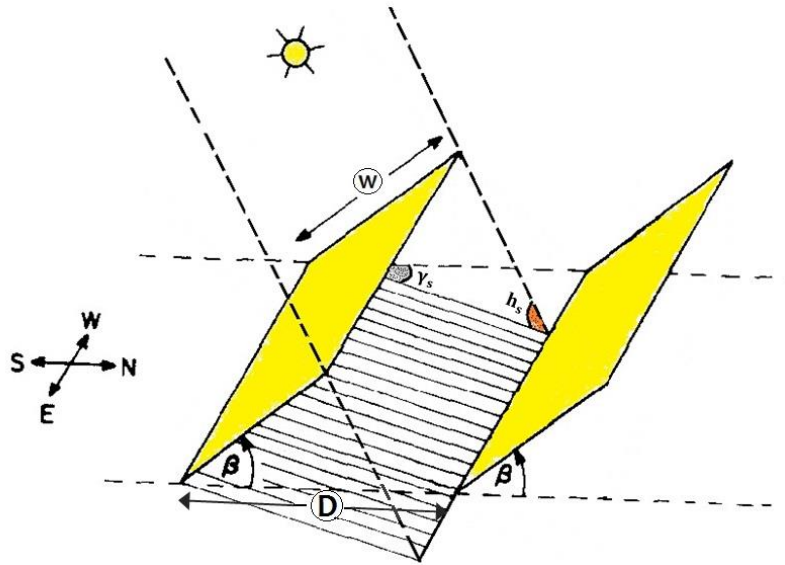
Figure 4.12: Inter-Row spacing variables.

Depending on the project variables, PV modules can be oriented either in landscape or in portrait. Landscape orientation of PV modules allows for a smaller gap between array positioning [24].

Dimensioning of the module rows can be done according to equinoxes and hours of a day. This means that from 21th March to 23rd September, during a predetermined time period in a day, the module rows should not be affected by self-shading.

In this study, spring equinox, 21th March was used as a dimensioning parameter. As can be seen from Table 4.3, distances between rows were calculated by Equation 4.2 with respect to the position of the Sun in given hours. 2.30 m were used as an inter-row spacing distance in simulations. Figure 4.13 (a) and (b) illustrate the PV modules layout on the roof.

Hours	Azimuth, γ_s (°)	Altitude, h_s (°)	Distance between rows, D (m)
09:00	-56	18	2.30
10:00	-41	24	2.28
11:00	-25	28	2.29
12:00	-8	31	2.25

Table 4.3: Calculated distances between rows with respect to azimuth and altitude of the Sun
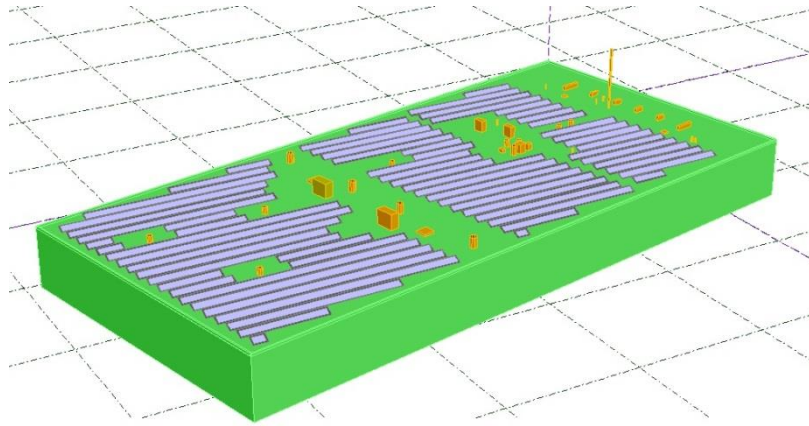
(a)
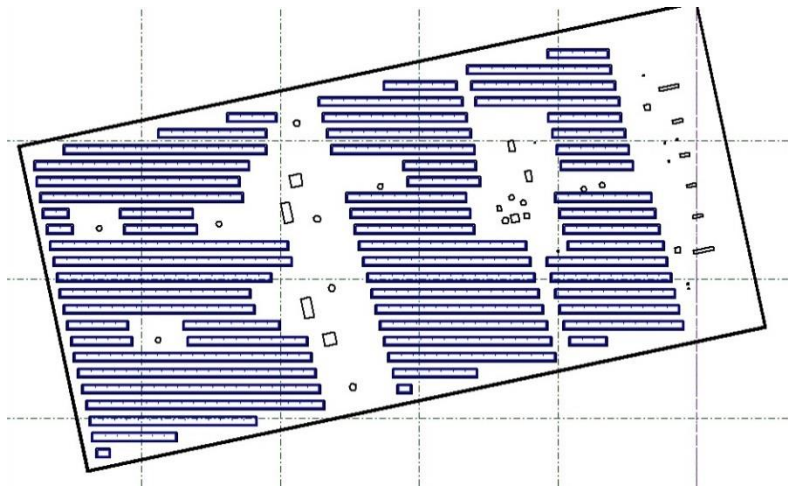
(b)

Figure 4.13: 3D illustration of PV modules layout (a) and (b)

4.7 Shading

Performance of PV systems is affected substantially as a result of shading on PV arrays. Losses caused by shading should be assessed by the way of taking two different kinds of losses into account. These are; *linear shading losses* which correspond to the deficit of irradiance on the cells and *electrical losses* resulting of the mismatch of electrical response of the modules in series and strings in parallel [20].

4.7.1 Electrical Effect of Shading

Shading on a cell or a group cells in a module reduces the total output power by causing mismatched cells. When the shaded cells get reverse-biased, the loss will be even more. As a general concept, the current of a module and a string with series connected cells and modules, respectively, is limited to the lowest current. As the shading on a cell or on a module reduces the current, this will lead cells or modules to be mismatched. On the other hand, shading on cells could result in hot-spot heating. One shaded cell in a series reducing the current through the good cells, leads them to produce higher voltages that can often reverse bias the bad cell. Power dissipation occurring in small area results in overheating which is called hot-spot heating and this might cause damages in the module. These unwanted effects of hot-spot heating can be avoided through the use of bypass diodes. It prevents large voltages from building up across the solar cells in the reverse-biased direction by diverting the current via a bypass which is provided by a bypass diode [17] (see Figure 4.14).
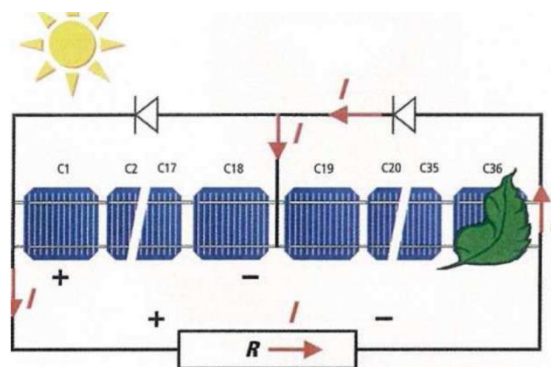
Figure 4.14: Bypass diode on solar cell [17]

In practice, bypass diodes are usually connected across 18 to 20 solar cells. Figure 4.15 shows the voltage current characteristics of a shaded module with and without a bypass diode.
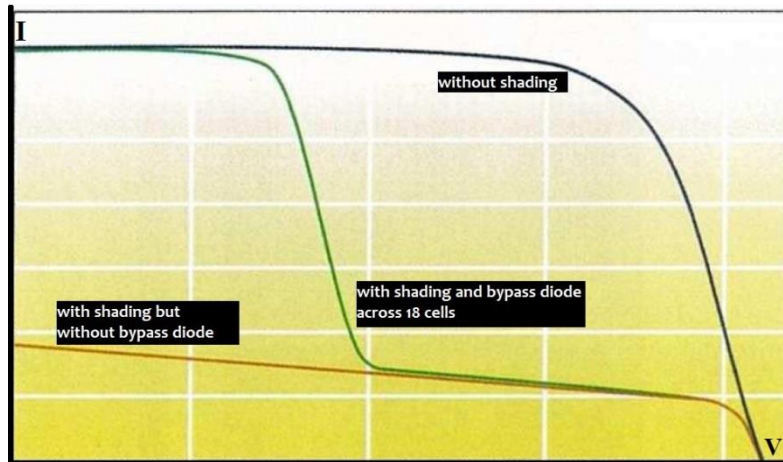
Figure 4.15: Module characteristic I-V curves with and without bypass diodes [17]

4.8 PVsyst Shading

Shading analysis is conducted based on two different types of shading in PVsyst. These are far shadings and near shadings.

4.8.1 Far Shadings

Far shading treatment consists of the shading objects sufficiently far away from the installation site and it is described by a horizon line. General consideration is that the distance of the shading objects should be higher than ten times the PV field size [20].

Far shading analysis is not a part of this study since the region is fairly flat, no mountains around and the structures are generally positioned at the north side of the site.

4.8.2 Near Shadings

Shadings resulted from near objects which draw visible shades on the PV array are considered as near shadings. PVsyst requires from the user to draw a detailed 3D description of the full PV system prior to the shading loss computation. Shading calculations are made for hourly steps during the simulation and applied on beam, diffuse and albedo components of near shading. Beam component is computed according to the direction of the sun as a function of azimuth and altitude angles while diffuse and albedo components are assumed to be constant during the year. Diffuse component is merely dependent on the system geometry. These

components of near shading are tabulated in the shading factor table with respect to the azimuth and altitude positions of the Sun. Shading factor is the "*shaded fraction of the PV field with respect to the full sensitive area [20].*"

For the beam component of near shadings two different kinds of losses are taken into account; linear shading losses (Irradiance losses) and electrical losses. As explained before, linear shading losses define the irradiance deficiency on the cells, as for the electrical losses, it represents the mismatch of electrical response of the array.

There are two options in PVsyst for assessing the electrical losses. These are:

Shading factor according to the module strings,
Detailed calculation according to the module layout.

Despite the fact that *the shading loss calculation according to the module layout* gives more detailed and accurate results since it requires all modules to be positioned on all shading areas; it is not required for big systems to be used [25]. Therefore, in this study, electrical losses were calculated by taking *shading factor according to the module strings* option into consideration.

When a PV cell is shaded, this will affect whole string current resulting in a non-linear effect on produced electricity. Due to the complexity of this phenomenon, PVsyst provides a simplified method which is called *shading factor according to the module strings.* This method assumes that when a string is partially shaded, the whole string is considered inactive in terms of beam component. This represents a higher limit on shading effect (100%). However, to be able to obtain more realistic results, *the fraction for electrical effect* should be specified. PVsyst recommends this value to be 100% where the shades are regular; 60 to 80% where the shades are distributed caused by shading objects such as chimneys and so on and for the thin objects it can be even less since the shade of a thin object will not cover a full cell [20].

Table 4.4 shows the assigned *fraction for electrical effect* values used in the simulations.

Fraction for electrical effect (shading objects)	Fraction for electrical effect (thin objects)
60%	40%

Table 4.4: Fractions for electrical effect used in simulations

4.9 PV Module Choice

PV module selection is an important step in system designing since the technical specifications of modules determines the rest of the system sizing. Modules can be chosen with respect to:

- Cell Material (mono-crystalline, polycrystalline, amorphous, CdTe or CIS, or thinfilm technology) and
- Module type (standard module with/without frames, glass-glass module, etc.) [17].

4.10 Sizing Inverters

4.10.1 Sizing Inverter According to the Power Specifications

The ratio between the PV array nominal power ($P_{nom(DC)}$) and the inverter nominal power output ($P_{nom(AC)}$) of 1:1 could be accepted as a general rule for sizing inverters when it comes to inverters power ratings. However, it is recommended to use a more reliable method for calculating required DC power by the way of dividing inverter nominal power($P_{nom(AC)}$ by inverter's nominal efficiency($\eta_{inv.}$). According to many inverters' technical specifications provided by manufacturers, $P_{nom(DC)}$ ratings are around 5 % higher than $P_{nom(AC)}$ on average.

Nevertheless, the inverter size is generally specified in the range of 0.8 to 1.2 to the array nominal power [17] (see Equation 4.3).

$$0.8 \times P_{nom(DC)} < P_{nom(AC)} < 1.2 \times P_{nom(DC)} \tag{4.3}$$

4.10.2 Sizing Inverter According to the Voltage Specifications

The sum of module voltages in a string is used for optimization according to the voltage ranges of inverters specified in technical data sheets privided by manufacturers. However, since the modules and PV array voltages changes depending on the ambient temperature values, minimum and maximum ambient temperatures are taken into account for determining the range of module numbers in a string. As is seen in Figure 4.16, the operating range of the inverter has to correspond to the PV array I/V curve and the MPP points of array I/V curve should not exceeds the admissible limits of the MPP range of the inverter at different temperatures.
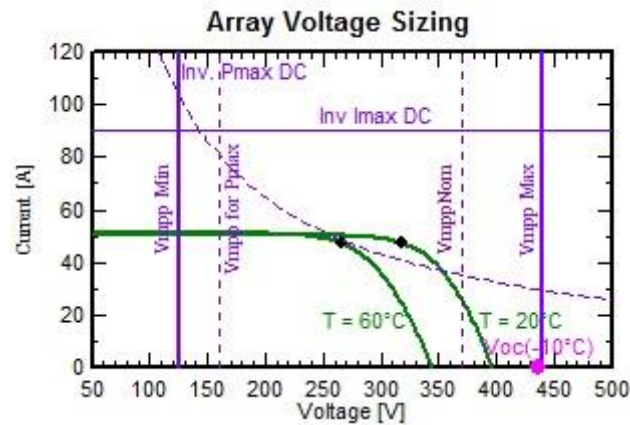
Figure 4.16: *PV array l-V curves and an inverter's operating range*

Minimum and maximum number of the modules in a string, (n_{min}) and (n_{max}) can be defined by the following equations, respectively [17].

$$n_{min} = \frac{V_{MPP(INV\ min)}}{V_{MPP(module\ max.temperature)}} \qquad (4.4)$$

$$n_{max} = \frac{V_{max(INV)}}{V_{OC(module\ min.temperature)}} \qquad (4.5)$$

where $V_{MPP(INV\ min)}$ is the minimum input voltage of the inverter at MPP and $V_{max(INV)}$ is maximum input voltage of the inverter.

Following terms, voltage of the module at MPP at the module maximum temperature $(V_{MPP(module\ max.temperature)})$ and open circuit voltage of the module at module minimum

42

temperature $(V_{OC(module\ min.temperature)})$ can be defined by the following equations, respectively [17] [26].

$$V_{MPP(module\ max.temperature)} = V_{MPP}(STC) \times \left[1 + \beta_{(V_{MPP})}(T_m - 25°C)\right] \quad (4.6)$$

$$V_{OC(module\ min.temperature)} = V_{OC}(STC) \times \left[1 + \beta_{(V_{OC})}(T_m - 25°C)\right] \quad (4.7)$$

where $V_{MPP}(STC)$ is the MPP voltage at STC, $V_{OC}(STC)$ is the open circuit voltage at STC, T_m is the module temperature, $\beta_{(V_{MPP})}$ and $\beta_{(V_{OC})}$ are the temperature coefficient values of V_{MPP} and (V_{OC}), respectively. Temperature coefficient is indicated as the voltage change in percentage per °C and prefixed with a negative sign.

4.10.3   Sizing Inverter According to the Current Specifications

Maximum PV array current should not be exceeding the maximum inverter input current $(I_{\max INV})$. Since the maximum PV array current is the sum of maximum string current, the maximum number of strings (n_{string}) should be less than or equal to the division of maximum inverter input current and maximum string current $(I_{max\ String})$ [17](see Equation 4.8).

$$n_{string} \leq \frac{I_{\max INV}}{I_{max\ String}} \quad (4.8)$$

4.10.4   Inverter Sizing in PVsyst

The inverter sizing principle in PVsyst is based on *acceptable overload loss* during an operation. For this reason, it takes the simulations in real conditions into account.

An acceptable Array-Inverter sizing in PVsyst is determined by perdefined parameters. According to this parameters if;

- *3% > Overload Loss > 0.2%* inverter slightly undersized (gives a warning)
- *Overload Loss > 3%* inverter strongly undersized (prevents the simulation).

"In practice these criteria leads to P_{nom} ratio ($P_{nom}array/P_{nom}inverter$) of the order of 1.25 to 1.3 for most well-oriented systems [20]."

4.11 Cable Sizing

Sizing DC cable is mainly done for keeping voltage drop (V_d) under a predefined loss limit. The main parameter for DC cables is the selecting proper cable material and cross section area of the cables.

First; the sample wiring schema of the array should be drawn for identifying the different parts of the circuits consisting of the module string connections to connection boxes and the connections between these boxes to inverters. Second; average cable lengths used in the array has to be measured for each circuit category and then, minimum required cable cross section size of cable is calculated for each parts of the circuit which is depended on the used material (usually copper or aluminum) on condition that voltage drop (V_d) should be kept under the predefined loss limit. Following equation is used for calculating minimum required cable cross section size(A_{DC}) :

$$A_{DC} = \frac{2.l_{DC}.\rho.I_{DC}}{V_d} \tag{4.9}$$

where I_{DC} is the string current, l_{DC} is the length of DC cable (multiplied by2, because there is always a return wire), V_d defines a loss in percentage with respect to the string voltage at MPP(V_{MPP}), ($V_d = Loss(\%) \times V_{MPP}$) and ρ is the resistivity of metals that is notably dependent on temperature as is seen from the equation 4.10 This equation represents a linear approximation providing that temperature (T) does not vary too much [20].

$$\rho(T) = \rho(T_0).[1 + \alpha_0.(T - T_0)] \tag{4.10}$$

where T_0 is any temperature used as a reference point, α_0 is the temperature coefficient of resistivity and $\rho(T_0)$ is the resisivity at temperature T_0.

4.12 Array Losses

All effects that reduce available array output energy corresponding with the PV module nominal power, indicated by the manufacturer at STC, can be named as array losses. After considering the irradiation shading effects (as explained in section 4.7), it is expected from an ideal PV array to yield $1kWh$ energy under $1kW$ irradiance at STC. Reduction in this ideal yield stems from several unavoidable losses.

PVsyst starts its loss evaluation from *the nominal energy, using the global effective irradiance and the array MPP nominal efficiency at STC* [20]. Then continues evaluating the each loss as a percentage of previous energy quantity.

After the simulation process in PVsyst, as can be seen from Figure 4.17, losses can be illustrated in a diagram.

|	
945 kWh/m²	Horizontal global irradiation
+18.6%	Global incident in coll. plane
-8.7%	Near Shadings: irradiance loss
-3.0%	IAM factor on global
-3.1%	Soiling loss factor
962 kWh/m² * 1103 m² coll.	Effective irradiance on collectors
efficiency at STC = 15.24%	PV conversion
161.8 MWh	Array nominal energy (at STC effic.)
-3.6%	PV loss due to irradiance level
-1.2%	PV loss due to temperature
-3.2%	Shadings: Electrical Loss acc. to strings
-0.7%	Module quality loss
-2.0%	LID - Light induced degradation
-2.0%	Module array mismatch loss
-0.7%	Ohmic wiring loss
141.0 MWh	Array virtual energy at MPP
-2.8%	Inverter Loss during operation (efficiency)
-0.0%	Inverter Loss over nominal inv. power
0.0%	Inverter Loss due to power threshold
0.0%	Inverter Loss over nominal inv. voltage
-0.0%	Inverter Loss due to voltage threshold
137.0 MWh	Available Energy at Inverter Output
137.0 MWh	Energy injected into grid

Figure 4.17: Shading Loss diagram in PVsyst

4.12.1 Thermal Losses

Reduction in a PV module performance is directly related to the module and ambient temperature. This correlation between ambient and increase in solar module temperature based on incident irradiance, representing the thermal energy balance, is given by the following equation in PVsyst:

$$U.(T_m - T_a) = \alpha.G_M.(1 - \eta) \tag{4.11}$$

where α is the irradiance global absorption coefficient of solar irradiation. 0.9 is the given default α value in PVsyst. However, it is possible to make change and designate another value instead. η is the PV efficiency related to the module area. PVsyst calculates η according to the operating conditions of the module when it is possible, if not 10% is used as default. U is the thermal loss factor that is used for characterizing the thermal behavior of the field, described by:

$$U = U_c + U_v.v \tag{4.12}$$

where U_c is the constant component and U_v is a factor proportional to the wind velocity v. These factors depend on the modules' mounting mode, sheds, roofing, facade, etc. PVsyst gives user an opportunity to determine the default value of the thermal loss factor U according to three different mounting options. In simulations, *free mounted modules with air circulation* option is set as default.

4.12.2 Ohmic Wiring Loss

PV Array Ohmic loss defines the power drop in an electrical circuit arising from circuit resistance and current flow. PVsyst, gives user an opportunity to compute the ohmic losses in three sections: DC circuit losses (ohmic losses for the array), AC circuit losses that occur from inverter to injection point (taken into account in case there is significant length of cable use) and external transformer losses. In scenarios, only DC circuit losses are taken into consideration since the AC cable lengths are not of significance to be counted in and external transformers are not used in the simulations.

The ohmic loss ratio is the ratio of wiring ohmic loss (P_w) compared to the array nominal power ($P_{nom}(array)$) (see Equations 4.13-4.14)

$$P_w = R_w . I_{SC}^2 \tag{4.13}$$

$$P_{nom}(array) = R_{array} . I_{SC}^2 \tag{4.14}$$

where R_w is the field global wiring resistance and R_{array} is the resistance $\left[V_{mp}/I_{mp} \right]$ at STC. In PVsyst, *"the global wiring resistance R_w of the system is obtained by putting all the sub-array wiring resistances in parallel [20]."* As the values of global wiring resistance and ohmic loss ratio are interrelated, it is possible to specify a target loss fraction in PVsyst. Proposed default value is given as 1.5% at STC and therefore, is used in the simulations.

4.12.3 Module Quality Loss

Module quality loss parameter represents a long term deviation of average effective module efficiency by respect to the manufacturer specifications. This parameter decreases the array P_{mpp} production at overall operating conditions in percentage.

PVsyst lets user specify any different value since the module quality loss parameter expresses user's own confidence to module performance. However, conducted studies on long term module performances in terms of degradation levels reported that in most cases, optimal value could be accepted as 0.7%/year for both monocrystalline and polycrystalline modules [27]. In the simulations, assigned module efficiency loss value has been taken as 0.7 %.

4.12.4 Light Induced Degradation (LID) Loss

Light Induced Degradation defines the power loss for crystalline silicon modules in the first operating hours of exposition to the Sun by respect to the manufacturing flash test values at STC. According to the reported studies [27], the values between 2% and 3% are reported in many cases. In PVsyst, 2% is accepted as a proposed default value to define LID loss factor and this value is used in the simulations.

4.12.5   Module Array Mismatch Loss

Considering the fact that the modules in an array do not have strictly identical I/V characteristics, this leads to mismatch losses. Because, as is known, the lowest module current drives the whole string current. PVsyst provides a statistical tool for estimating the mismatch loss for the cells in a module or the modules in an array. This tool first creates a statistical sample of modules with reference to the mismatched module parameters I_{SC} and V_{OC} through Gaussian or square distribution, then draws the array I/V curve by adding each voltage and current value of the array, and then identifies the MPP which is possible to compare with the MPP value of the array with identical modules. Each run of the tool, results vary due to the statistical approach. However, PVsyst creates a histogram by operating great number of statistical samples and this is used for estimating the mismatch loss parameter, which has to be specified by the user as an input parameter [20]. This parameter has to be in an acceptable range, "*the typical manufacturing tolerance of PV module output power is* $+/-3\%$ *[28]*". After running the simulations in PVsyst, proposed default value of the mismatch losses has been specified and used in the simulations.

4.12.6   Soiling Loss

Soiling Loss corresponds to the irradiance loss due to dust, snow, bird droppings and any kind of dirt on photovoltaic modules. It is not easy to estimate the accumulation of dirt and its effect on module performance owing to the varying environment of the system, raining and snowing conditions. However, many studies which have been conducted in different geographical locations and climate conditions let us estimate the value of yearly soiling loss factor [27].

On account of the fact that presence of snow and its effects in winter seasons in Estonia is of significance, snow is considered as a soiling factor and specified in PVsyst by the way of defining loss factors in monthly values. Figure 4.18 shows the monthly soiling values used in simulations.

Figure 4.18: Monthly soiling values used in simulations

4.12.7   Array Incidence Loss (IAM)

The incidence effect or *Incidence Angle Modifier (IAM)* defines the reduction in irradiance level hitting on the surface of photovoltaic cells according to the nominal conditions, considering the fact that increment in incidence angle (defining the angle of the Sun rays with respect to the normal to the collector plane) is proportionate to the amount of reflected irradiation from the surface of the module. The light reaching the cell's surface under the glass which is frequently used as a protective layer mainly depends on characteristic refraction index of used material and the angle of incidence.

In PVsyst, ASHRAE model is used as a parameterization method depending on only one coefficient value (b_0). Following equation is often used for computing the Incidence Angle Modifier Factor(F_{IAM}).

$$F_{IAM} = 1 - b_0 \left(\frac{1}{\cos i} - 1 \right)$$
(4.15)

where i is the incidence angle on plane. Assigned PVsyst b_0 values for crystalline and single-glazed thermal solar modules are 0.05 and 0.1, respectively.

4.12.8   Irradiance Level Loss

Efficiency of a module decreases for lower irradiances. PV array loss due to the irradiance level describes the degradation of module efficiency according to the decrease in irradiance level with respect to the efficiency of a module at STC. The intrinsic behavior of PV modules

leading to the loss due to irradiance level is described by taking two parameters into account for standard one-diode model in PVsyst; one of which is the shunt resistance exponential behavior (RshExp) and the other is series resistance (Rserie). While the shunt resistance increases exponentially in case of reduced irradiation level with respect to the STC, series resistance goes with the square of the current. Therefore, to be able to get higher performances under low irradiance conditions, modules should have low shunt and high series resistance.

4.12.9   Shading Losses

Performance of PV systems is affected substantially as a result of shading on PV arrays. Losses caused by shading should be assessed by the way of taking two different kinds of losses into account. These are; *linear shading losses* which correspond to the deficit of irradiance on the cells and *electrical losses* resulting of the mismatch of electrical response of the modules in series and strings in parallel [20].

Due to the fact that a variety of factors have a role in shading losses calculations, this subject is discussed in section 4.7 in detail.

5.   System Performance

In order to assess the overall performance of PV Systems and make comparisons between different scenarios, following derived parameters are taken into account with respect to IEC *61724 Photovoltaic System Performance Monitoring – Guidelines for Measurement, Data Exchange and Analysis* norms [29].

IEC 61724 Performance Indices indicated in PVsyst software are:

Reference System Yield (Y_r)
Array Yield (Y_a)
System Yield (Y_f)
Collection Loss (Y_c)
System Loss (L_s)
Performance Ratio (PR)

These normalized indicators - taking into account the array nominal installed power at STC (P_{nom}) - are correlative to the incident global irradiation in the collector plane (GlobInc). Therefore, these indicators enable designers to assess PV systems independently from the array size, the geographic situation and orientation of the field. The yield energies in the performance indices are stated in the unit of $kWh/kWp/day$, and also can be expressed as *hours/day* when running at $1kW/m^2$ or $kWh/m^2/day$ due to the fact that they are equal to the *equivalent operating time* under a constant irradiance of $1kW/m^2$ [20].

5.1   Reference System Yield

Reference System Yield (Y_r) is defined in PVsyst 6 User's Guide as ideal array yield on the basis of array nominal installed power at STC, regarding that the array operates without any loss. From a different viewpoint, it expresses that the array nominal power during one hour should be tantamount to each incident *kWh*. Y_r is numerically equal to the incident energy in the array. However, it can be expressed as either the ideal array yield according to P_{nom} *(kWh/kWp/day)* or the incident energy *(kWh/m²/day)*. Unit of Y_r is indicated as *kWh/m²/day* in PVsyst.

5.2 Array Yield

Array Yield (Y_a) is the array daily output energy as part of the nominal power. Unit of Y_a is indicated as $kWh/kWp/day$ in PVsyst.

5.3 System Yield

System Yield (Y_f) is the total useful energy produced by the system per day, week, month or year as part of the nominal power. Unit of Y_f is indicated as $kWh/kWp/day$ and $kWh/kWp/year$ (named as specific production in final report sheet) in PVsyst.

5.4 Collection Loss

Collection Loss (L_c) represents array losses, taking into account thermal, ohmic, module quality, mismatch, incidence (IAM), shading, soiling, MPP, regulation losses and all other inefficiencies. L_c is the difference between Reference System Yield (Y_r) and Array Yield (Y_a) indicated below:

$$L_c = Y_r - Y_a \qquad (5.1)$$

5.5 System Loss

System Loss (L_s) include inverter loss in grid-connected systems, or battery inefficiencies in stand-alone as defined in PVsyst 6 User's Guide. L_s is the difference between Array Yield (Y_a) and System Yield (Y_f) indicated below:

$$L_s = Y_a - Y_f \qquad (5.2)$$

5.6 Performance Ratio

One of National Renewable Energy Laboratory (NREL) based scientific paper [30] defines Performance Ratio as follows: *"The performance ratio PR is the Y_f divided by the Y_r. By normalizing with respect to irradiance, it quantifies the overall effect of losses on the rated output due to: inverter inefficiency, and wiring, mismatch, and other losses when converting from DC to AC power; PV module temperature; incomplete use of irradiance by reflection*

from the module front surface; soiling or snow; system down-time; and component failures."
It is seen that PR is a useful parameter to evaluate both different systems in same location and similar systems in different geographical locations by virtue of the fact that it is normalized.

In PVsyst 6 User's Guide [20], Performance Ratio is defined as the global system efficiency concerning the nominal installed power and the incident energy and it is equal to the System Yield (Y_f) divided by the Reference System Yield (Y_r). It can be expressed by the following equation [20]:

$$PR = \frac{Y_f}{Y_r} \ (dimensionless) \tag{5.3}$$

As a dimensioning criterion, it can be assumed that PR should be higher than 70% [17].

6.   Simulations and Results

This section includes;

- classification of the simulations,
- the main simulation parameters,
- comparison of different scenarios depending on the loss and performance results,
- determining the best design choice according to the performance results,
- making comparison between monthly energy consumption of the building and energy production of the selected design which provides the best performance,
- general discussion on the results.

Simulations were performed in four main section based on the selected technology (PV modules and inverter) and each simulation was performed six times by changing only the plane tilt from the optimum tilt angle 39˚ to 10˚, which are 39˚, 30˚, 25˚, 20˚, 15˚ and 10˚. These are named as "scenarios" as seen in Table 6.1. To put it another way, consequently, 24 different simulations were taken into account in order to make performance analyses in this study.

PV modules and inverters used in the simulations are:

PV modules:

- Sharp ND-R250A5   (Polycrystalline)
- Sharp NU-R250J5   (Mono-crystalline)

Inverters:

- PLATINUM 13000 TLD
- Huawei Tech. SUN2000-28k
- Samil Power Solar Lake 25000TL-PM

Technical Specifications of the inverters and the PV modules are available at Appendix 1.

Table 6.1 combined:

Simulation name	Simulation Technology Module / Inverter		Scenario number	Module tilt angle (°)		Scenario name
P1	(Polycrystalline) Sharp ND-R250A5 PLATINUM 13000 TLD		1	39		P1-1
			2	30		P1-2
P2	(Polycrystalline) Sharp ND-R250A5 Huawei Tech. SUN2000-28k		3	25		P1-3
			4	20		P1-4
M1	(Monocrystalline) Sharp NU-R250J5 PLATINUM 13000 TLD		5	15		P1-5
			6	10		P1-6
M2	(Monocrystalline) Sharp NU-R250J5 SamilPower SolarLake 25000TL-PM					P2-1
						P2-2
						•
						•

Table 6.1: Classification of the simulations

Table 6.2 gives the total number of modules, inverters, modules in series and strings in parallel according to the simulations

Simulation name:	P1	P2	M1	M2
Module	(Polycrystalline) Sharp ND-R250A5		(Monocrystalline) Sharp NU-R250J5	
Inverter	PLATINUM 13000 TLD 749842	Huawei Tech. SUN2000-28k TL	PLATINUM 13000 TLD 749842	Samil Power Solar Lake 25000TL-PM
Total number of modules	672	684	684	684
Total number of inverters	12	6	12	6
Number of modules in series	14	19	19	19
Number of strings in parallel	48	36	36	36

Table 6.2: Simulations settings

6.1   Simulation Parameters

Simulation parameters are stated in Tables 6.3, 6.4, 6.5, 6.6 and 6.7.

Table 6.3 : Orientation Parameters	
Field Type	Fixed tilted plane
Azimuth	0˚
Plane Tilt	39˚, 30˚, 25˚, 20˚, 15˚, 10˚
Inter-Row Spacing (pitch)	2.30 m

Table 6.4: Module Loss Parameters	
Module Quality Loss	0.7%
Light Induced Degradation (LID)	2%
Module Array Mismatch Loss	2%

Table 6.5: Soiling Loss Parameters					
January	February	March	April	May	June
30%	30%	2%	2%	2%	2%
July	August	September	October	November	December
2%	2%	2%	2%	2%	20%

Table 6.6: DC Cable Loss Parameters							
Simulation name	String module connections		Main box to inverter		Total copper mass [kg]	Field global wiring resistance [$mOhm$]	Wiring loss fraction at STC [%]
	Average length per circuit[m]	Cross Section Area (CSA)[mm^2]	Average length per circuit[m]	Cross Section Area (CSA)[mm^2]			
P1	80	2.5	30	16	121	15.5	1.4
P2	105	2.5	30	16	97	27.8	1.4
M1	105	2.5	30	6	91	29.8	1.5
M2	105	2.5	30	16	97	27.8	1.4

Table 6.7: Shading Loss Parameters (electrical)	
Fraction for electrical effect (shading objects)	Fraction for electrical effect (thin objects)
60%	40%

6.2 Results

6.2.1 System Losses

Tables 6.8, 6.9, 6.10 and 6.11 give the losses in percentage of each scenario.

Table 6.8: SIMULATION-P1 SYSTEM LOSSES (%)						
Scenario Name	P1-1	P1-2	P1-3	P1-4	P1-5	P1-6
Module Tilt Angle	**39°**	**30°**	**25°**	**20°**	**15°**	**10°**
Shading loss (linear)	-8.7	-5.9	-4.3	-2.9	-1.9	-0.9
Shading loss (electrical)	-3.2	-2.8	-2.0	-1.2	-0.5	-0.4
Soiling loss	-3.1	-3.1	-3.1	-3.1	-3.0	-3.0
IAM	-3.0	-3.1	-3.3	-3.5	-3.8	-4.2
Irradiance Level Loss	-3.6	-3.6	-3.7	-3.7	-3.9	-4.0
Thermal Loss	-1.2	-1.1	-1.0	-0.9	-0.7	-0.4
Ohmic Loss	-0.7	-0.7	-0.7	-0.7	-0.7	-0.6
Module Array Mismatch Loss	-2.0	-2.0	-2.0	-2.0	-2.0	-2.0
LID	-2.0	-2.0	-2.0	-2.0	-2.0	-2.0
Module quality loss	-0.7	-0.7	-0.7	-0.7	-0.7	-0.7
Inverter loss	-2.8	-2.8	-2.8	-2.8	-2.8	-2.8

Figure 6.1 shows the changes in losses (except module mismatch, quality and LID) according to the module tilt angles concerning the simulation P1. (It is not necessary to apply this graph for other simulations since it is fairly the same).

As is seen from Figure 6.1, linear shading loss and together with the electrical loss caused by shading increase substantially along with the increase in module tilt angles. Thermal loss

shows a slight increase from 0.4% to 1.2% as the module tilt increases. As for IAM and Irradiance level loss, it can be said that there is a reverse relation with the increase in module tilt angles. IAM and Irradiance level loss decrease from 4.2% to 3.0% and from 4.0% to 3.6%, respectively.
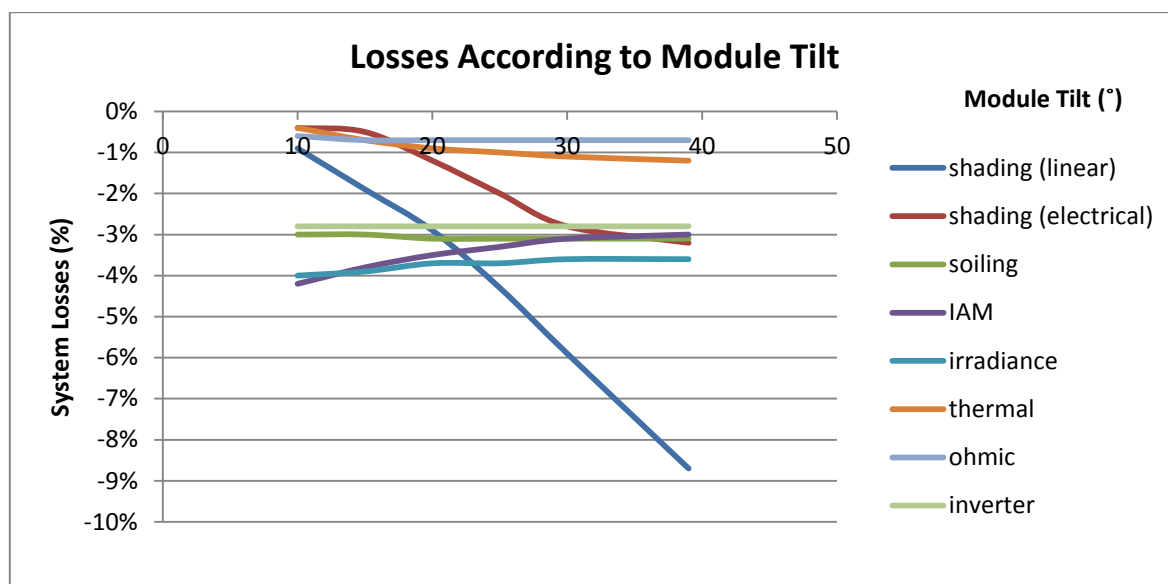

Figure 6.1: Simulation-P1 Losses according to module tilt

Table 6.9: SIMULATION-P2 SYSTEM LOSSES (%)						
Scenario Name	P2-1	P2-2	P2-3	P2-4	P2-5	P2-6
Module Tilt Angle	**39°**	**30°**	**25°**	**20°**	**15°**	**10°**
Shading loss (linear)	-8.7	-5.9	-4.3	-2.9	-1.9	-0.9
Shading loss (electrical)	-3.2	-2.7	-2.0	-1.2	-0.5	-0.4
Soiling loss	-3.1	-3.1	-3.1	-3.1	-3.0	-3.0
IAM	-3.0	-3.1	-3.3	-3.5	-3.8	-4.2
Irradiance Level Loss	-3.6	-3.6	-3.7	-3.7	-3.9	-4.0
Thermal Loss	-1.2	-1.1	-1.0	-0.9	-0.7	-0.4
Ohmic Loss	-0.7	-0.7	-0.7	-0.7	-0.7	-0.6
Module Array Mismatch Loss	-2.0	-2.0	-2.0	-2.0	-2.0	-2.0
LID	-2.0	-2.0	-2.0	-2.0	-2.0	-2.0
Module quality loss	-0.7	-0.7	-0.7	-0.7	-0.7	-0.7
Inverter loss	-2.6	-2.5	-2.5	-2.5	-2.5	-2.5

Table 6.10: SIMULATION-M1 SYSTEM LOSSES (%)						
Scenario Name	M1-1	M1-2	M1-3	M1-4	M1-5	M1-6
Module Tilt Angle	**39°**	**30°**	**25°**	**20°**	**15°**	**10°**
Shading loss (linear)	-8.7	-5.9	-4.3	-2.9	-1.9	-0.9
Shading loss (electrical)	-3.3	-2.8	-2.0	-1.2	-0.6	-0.4
Soiling loss	-3.1	-3.1	-3.1	-3.1	-3.0	-3.0
IAM	-3.0	-3.1	-3.3	-3.5	-3.8	-4.2
Irradiance Level Loss	-3.1	-3.1	-3.1	-3.2	-3.3	-4.4
Thermal Loss	-1.3	-1.2	-1.1	-0.9	-0.7	-0.5
Ohmic Loss	-0.8	-0.8	-0.8	-0.8	-0.7	-0.7
Module Array Mismatch Loss	-2.0	-2.0	-2.0	-2.0	-2.0	-2.0
LID	-2.0	-2.0	-2.0	-2.0	-2.0	-2.0
Module quality loss	-0.7	-0.7	-0.7	-0.7	-0.7	-0.7
Inverter loss	-2.8	-2.8	-2.8	-2.8	-2.8	-2.8

Table 6.11: SIMULATION-M2 SYSTEM LOSSES (%)						
Scenario Name	M2-1	M2-2	M2-3	M2-4	M2-5	M2-6
Module Tilt Angle	**39°**	**30°**	**25°**	**20°**	**15°**	**10°**
Shading loss (linear)	-8.7	-5.9	-4.3	-2.9	-1.9	-0.9
Shading loss (electrical)	-3.3	-2.8	-2.0	-1.2	-0.6	-0.4
Soiling loss	-3.1	-3.1	-3.1	-3.1	-3.0	-3.0
IAM	-3.0	-3.1	-3.3	-3.5	-3.8	-4.2
Irradiance Level Loss	-3.1	-3.1	-3.1	-3.2	-3.3	-3.4
Thermal Loss	-1.3	-1.2	-1.1	-0.9	-0.7	-0.5
Ohmic Loss	-0.7	-0.7	-0.7	-0.7	-0.7	-0.6
Module Array Mismatch Loss	-2.0	-2.0	-2.0	-2.0	-2.0	-2.0
LID	-2.0	-2.0	-2.0	-2.0	-2.0	-2.0
Module quality loss	-0.7	-0.7	-0.7	-0.7	-0.7	-0.7
Inverter loss	-2.7	-2.7	-2.7	-2.6	-2.6	-2.6

Table 6.12 shows the increase in global incident in collector plane with respect to the horizontal global irradiation as the module tilt angle increases. PVsyst starts its loss evaluation first by adding the global addition onto the horizontal global irradiation and then continues with the losses process.

Table 6.12: Global incident in collector plane						
Module Tilt Angle (˚)	39°	30°	25°	20°	15°	10°
Global incident in collector plane [global addition] (%)	+18.6	+17.5	+16.0	+14.0	+11.3	+8.0

6.2.2 Produced Energy, Specific Production and Performance Ratio

Table 6.13 gives the energy production, specific production and performance ratio results of the scenarios. As can be seen, the highest PR values belong to 10˚ tilted scenarios. On the other hand, 20˚ tilted orientation based scenarios give the highest values among all in specific production and produced energy.

Module / Inverter	Simulation name	Scenario number	Module tilt angle (°)	Produced energy (MWh/year)	Specific production (kWh/kWp/year)	Performance Ratio (PR) (%)
(Polycrystalline) Sharp ND-R250A5 PLATINUM 13000 TLD 749842	P1	1	39°	137.0	816	72.8
		2	30°	140.8	838	75.5
		3	25°	142.2	847	77.2
		4	20°	**142.7**	**849**	78.9
		5	15°	141.6	843	80.1
		6	10°	138.6	825	**80.8**
(Polycrystalline) Sharp ND-R250A5 Huawei Tech. SUN2000-28k TL	P2	1	39°	139.7	817	72.9
		2	30°	143.5	839	75.6
		3	25°	145.0	848	77.4
		4	20°	**145.5**	**851**	79.0
		5	15°	144.4	844	80.3
		6	10°	141.3	827	**81.0**
(Monocrystalline) Sharp NU-R250J5 PLATINUM 13000 TLD 749842	M1	1	39°	140.1	819	73.1
		2	30°	143.9	841	75.8
		3	25°	145.4	850	77.6
		4	20°	**145.9**	**853**	79.2
		5	15°	144.8	847	80.5
		6	10°	141.8	829	**81.2**
(Monocrystalline) Sharp NU-R250J5 Samil Power Solar Lake 25000TL-PM	M2	1	39°	139.9	818	73.0
		2	30°	143.7	840	75.7
		3	25°	145.3	850	77.5
		4	20°	**145.8**	**853**	79.2
		5	15°	144.7	846	80.4
		6	10°	141.7	829	**81.2**

Table 6.13: Performance Results of the Scenarios

Selection of the Best Design

Commonly used determiner to evaluate system performances is PR, however, PR is more useful for comparing PV systems at different locations [17]. Therefore, yearly specific yield (specific production) is used to determine the best performing system. In comparison with the specific productions of the scenarios, it is seen that the scenario M1-4 with 20° module tilt gives the highest value among all scenarios.

Figure 6.2 and 6.3 show the monthly PR and normalized production and loss factors of scenario M1-4 in percentage, respectively.

Performance Ratio PR
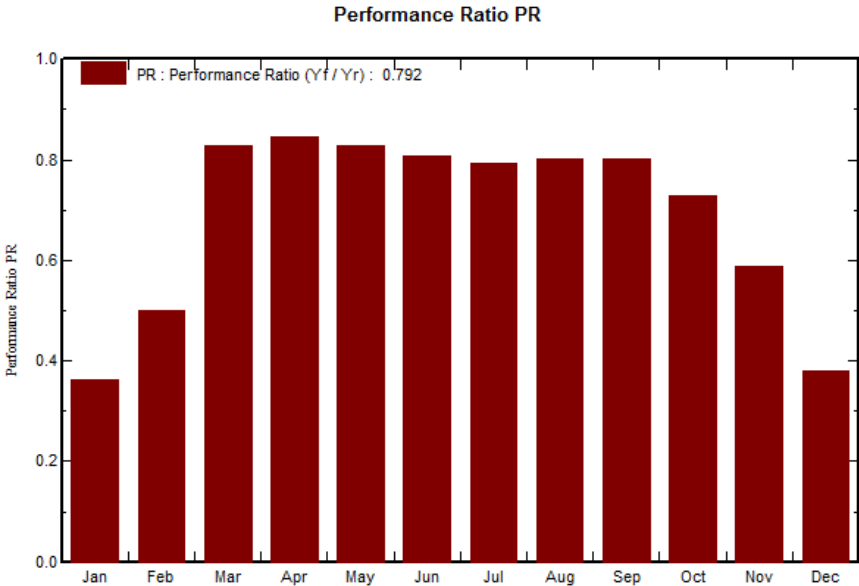
Figure 6.2: Scenario M1-4 monthly performance ratios

Normalized Production and Loss Factors: Nominal power 171 kWp
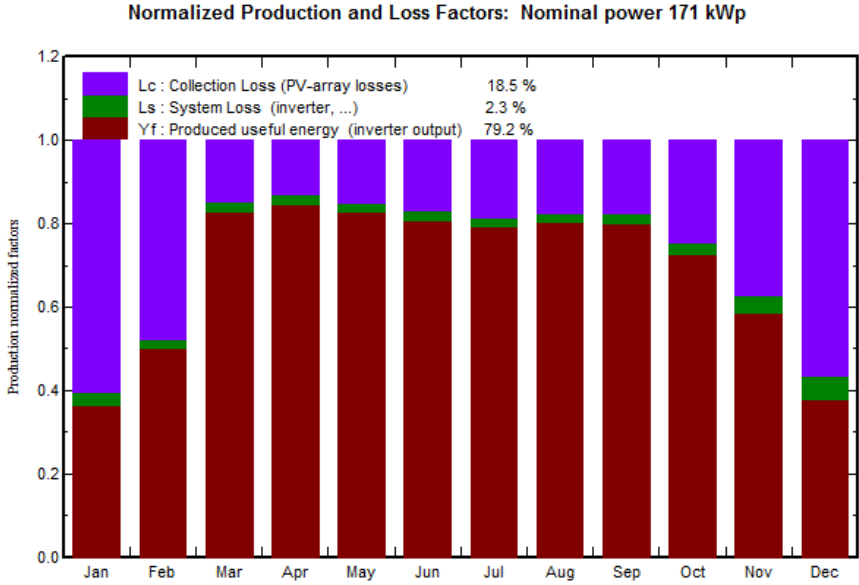

Figure 6.3: Scenario M1-4 monthly normalized production and loss factors

6.2.3 Discussion on Results

As is seen in Table 6.8, 6.9, 6.10 and 6.11 shading loss decreases with decreasing module tilt angle. The main reason is that because the distance between rows maintained at 2.30 m as the tilt angle of modules altered. Therefore, shading caused by the tilt angle, in other saying, the height of the modules sweeps less amount of area. This results in that the shading loss together with electrical loss stemming from shading decrease with decrease in tilt angle.

As for Table 6.13, specific production decreases from the tilt angle 20° to 10°. The reason for that can be explained by the effects of global addition on collector plane and shading losses. The sum of these values represents fairly the same proportional trend with the specific production numbers.

6.3 Energy Production and Consumption

Table 6.14 shows the monthly electrical energy consumption of the building and production results. The production results belong to the Scenario M1-4 which is determined as the best performing system design. Monthly energy consumption values belong to year 2013.

Table 6.14: Monthly Energy Consumption and Production			
	Energy Consumption (2013) (kWh/month)	Energy Production (kWh/month)	% of 2013 consumption
January	36194	671	1.85%
February	33313	2688	8.07%
March	33357	11497	34.47%
April	33636	17736	52.73%
May	29528	24863	84.20%
June	23482	25831	110.00%
July	24581	24032	97.77%
August	21051	19591	93.06%
September	28231	11951	42.33%
October	32452	5431	16.74%
November	35887	1229	3.42%
December	36275	387	1.07%
Year	367987 kWh/year	145907 kWh/year	39.65%

Figure 6.4 shows the monthly production and 2013 consumption of the system.
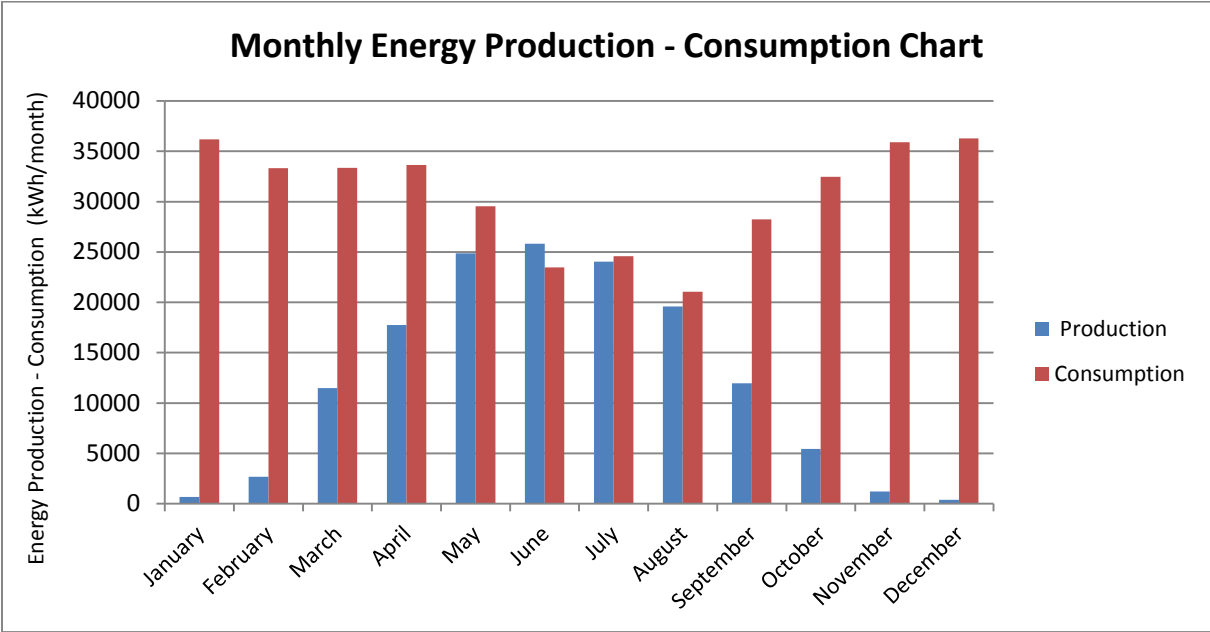
Figure 6.4: Monthly energy production and consumption

6.3.1 Discussion on Energy Production and Consumption

As shown in Table 6.4, selected system (M1-4) energy production covers almost 40% of the total yearly electrical energy consumption of the building in 2013.

When taking Figure 6.4 into consideration, it can be said that monthly energy production and consumption distribution represents an inverse correlation. As the need for energy of the building increases in winter time, energy production decreases. Energy production during June is the only one which exceeds the monthly electrical energy consumption of the building.

7. Economics

7.1 Theory

There are many methods which are used for economic performance evaluation, such as Levelized Cost of Energy (LCOE), Net Present Value (NPV), Internal Rate of Return (IRR), Simple and Discounted Payback methods. The Simple Payback method is known as the most simplistic method among others.

Simple payback is a frequently used method for evaluating economic performance of investments, especially in the field of energy. It is defined as the number of years to cover the cost of an investment. Simple payback is a simplistic method which is mainly used for preliminary estimations since some determinants such as the time value of money and cash flows after the payback period are not taken into account. If the simple payback period is not in acceptable limits and too much to be compared to the lifetime of the project, there will be no need to go further. As is seen from Equation 7.1, simple payback time (SP) can be calculated by dividing initial cost of a project by annual expected savings [31].

$$SP = \frac{Project\ Initial\ Cost}{Annual\ Expexcted\ Savings} \tag{7.1}$$

where SP is the simple payback period. Annual Expected Savings can be calculated by multiplying estimated annual energy production and grid price per energy unit [32].

7.2 Methodology

Economic evaluation of the project is conducted by comparing the life time of the project (20 years) and simple payback time.

Project initial cost can be separated into two parts; first BoS and installation costs and second PV module cost.

BoS and installation costs include basically inverters, mounting and racking system components, combiner boxes, electrical components, labor, battery storage for off-grid systems and system design and management costs [33].

65

The cost of BoS components and installation largely depend on the size and the type of installation. From utility scale grid-connected PV plants to the off-grid systems, it may range from 20% to 70% of total initial costs.

Figure 7.1 shows the PV module, BoS and installation cost distributions for both ground-mounted and rooftop systems in the United States by 2010. As for rooftop designs, BoS total cost per Wp is 1.85 USD, accounting for 49% and PV module cost is 1.9 USD/Wp, corresponding to 51% of the total PV system cost, 3.75 USD.

In this study, 49%-51% was used as a dimensioning scale in order for determining the cost of installation and BoS components according to the PV module prices.
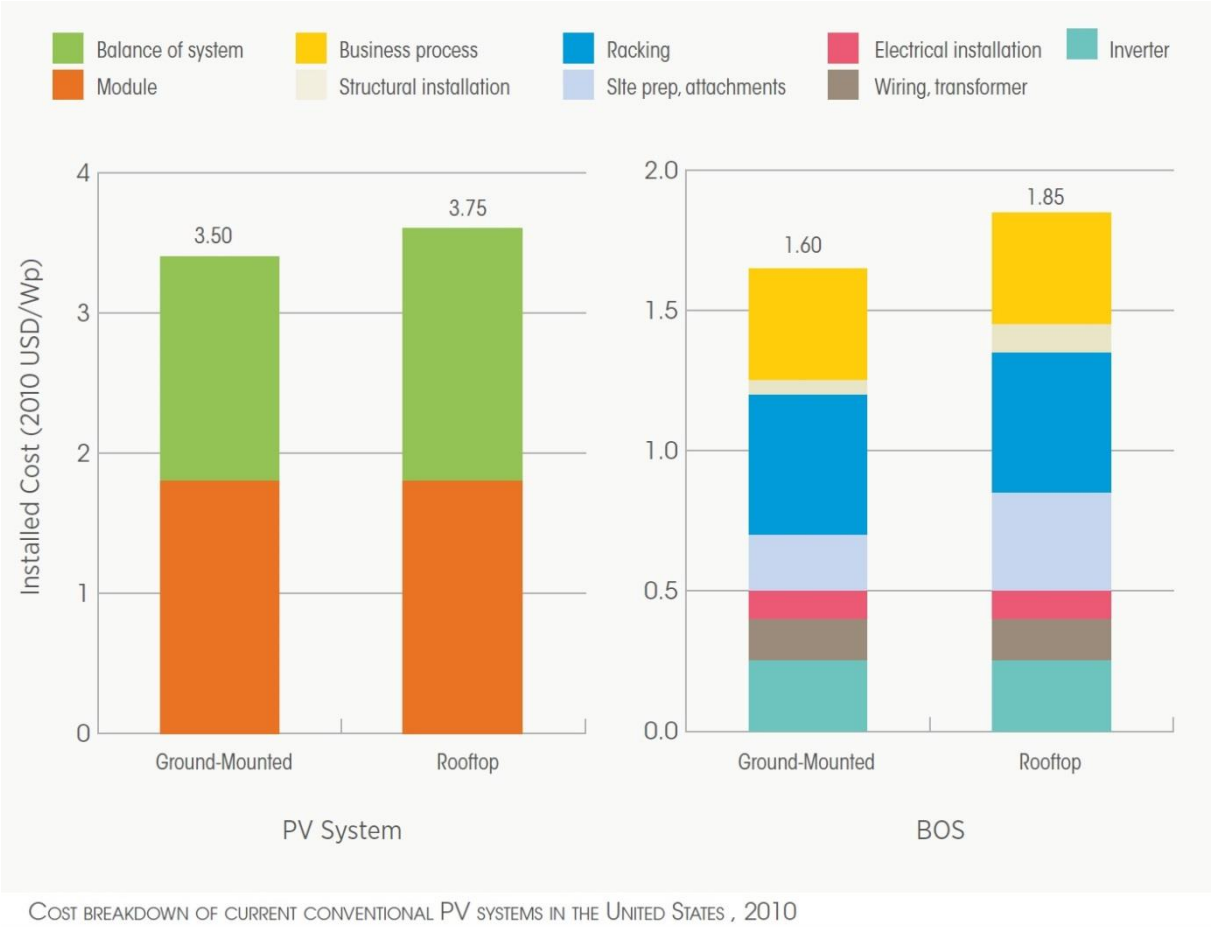
Figure 7.1: Cost distribution of PV systems in the US by 2010 [33]

The simple payback periods of simulated designs were calculated within the scope of two different cases scenarios, which are the best case and conservative case.

For the best case scenario, Crystalline silicon PV module average price in 2014 is determined by taking module price projection table into account that assumes a drop in module and as for the conservative case scenario, it was assumed that the average price of a Crystalline silicon PV module in 2012 maintains its price until the end of 2014 (see Appendix 2). As the prices in the tables are in the USD currency, they were converted to Euro currency in calculations (rate 0.733 USD/Euro by May 31st 2014).

Grid price for renewable energies in Estonia is 0.0537 euros/kWh [34].

For the best case scenario, PV module price is around 0.682 euros/Wp, BoS is around 0.655 euros/Wp, in total 1.337 euros/Wp. For the conservative case scenario, PV module price is around 0.894 euros/Wp, BoS is around 0.859 euros/Wp, in total 1.753 euros/Wp.

7.3   Results

Simple payback periods were calculated by taking only the best performed scenario (M1-4) into   account$(P_{nom}total = 171\,kWp, Produced\,Energy = 145.9MWh/year)$.   Table   7.1 gives the results for two cases. As is seen, simple payback times for both cases are largely higher than the project life time 20 years.

Table 7.1: Project Initial Costs and Simple Payback Periods		
	Best Case	Conservative Case
Lifetime of the project (years)	20	20
Project Initial Cost (euros)	228567	299840
Simple Payback Time (years)	29.17	38.26

7.4   Discussion on Economics

Simple payback method has its own limitations on economic evaluation of a system since many factors are not included in it. Therefore, using different economic evaluation methods may be more preferable for such systems. However, in this study, as mentioned before, simple payback method is used as a first step to be able to determine the boundaries from the point of

economics. Since the simple payback periods represented largely higher values than life time period of the project, there is no need to go further.

On the other hand, one of the most important determiners in simple payback calculations is the grid price for renewable energies in Estonia, 0.0537 euros/kWh since 2008. Since that time, the basic tariffs have been set on this number [35]. In case the grid price increases in near future, this may turn the tables on.

8. Conclusion

The thesis comprises the basic processes for designing a suiting PV design on a flat roof. As the roof is flat and there are shading objects on it, the process starts with determining the optimum tilt angle at Tallinn. The distance between rows was determined by taking the spring equinox into account with the hour range from 09.00 to 15.00. Consequently it was assumed that the rows would not shade each other between 9 am to 3 pm during six months from March 21st to September 23rd. In addition, plenty number of different shading objects were also taken into account for placing the rows properly.

Two different PV modules and three inverters were chosen to be used in the simulations which are; Sharp ND-R250A5 (polycrystalline) and NU-R250J5 (mono-crystalline), as for the inverters, PLATINUM 13000 TLD, Huawei Tech. SUN2000-28k and Samil Power Solar Lake 25000TL-PM. Incident irradiation is not very high at Tallinn since it is located at north. Therefore, a special attention was paid for choosing PV modules which has higher MPP at lower irradiance levels. As for the inverters, they were chosen mostly according to the efficiencies and sizes.

Simulations were performed in four section based on the technology matching of the PV modules and inverters. By taking the inter-row spacing fixed at 2.30m which was calculated for the optimum tilt angle 39˚, the module tilt angle was altered to lower degrees in order to increase the system performance. Consequently, the best performing system has been determined as the system with 20˚ tilt angle with 853 kWh/kWp/year specific production and with 145.9 MWh/year energy production. However, this amount of production could cover only 39.65% of electrical energy consumption of the TUT Sports Center Building.

From an economic point of view, it was seen that it is not profitable to invest these designs since the grid price is not enough to compensate for the initial investment cost.

9. Resume

This thesis focuses on designing a suiting grid-connected photovoltaic system for the flat roof of Tallinn University of Technology Sports Center Building, consisting of geographical location parameters, meteorological data, PV module orientation, PV modules and inverters selection, sizing the array in accordance with the inverters' specifications, cable sizing, shading analysis, detailed loss and performance analyses and performing different scenarios with differently matched technologies and plane orientations.

The thesis should be considered as a preliminary study of a grid-connected system design since it focuses mainly on the electrical behavior of the system; apart from that some assumptions were made in a few calculation processes such as average lengths of the cables which is used in the simulations.

PVsyst software program was used in this study as a support tool. The extensive functionality and complexity of PVsyst makes it one of the most comprehensive programs. It is used by architects, scientists, engineers and PV specialists all around the world. Module characteristic curves calculation, partial and 3D shading analysis, importing system measurement data and many other features can be performed in PVsyst.

Synthetic meteorological data creation, optimal orientation of the PV modules, inverter sizing, loss parameters and linear and electrical effects of shading were determined and performed by PVsyst in the thesis.

Simulations in the study were performed with different PV modules, inverters and different plane orientations in order to observe the alteration in performance ratios, specific yields and the amount of annual energy production. Consequently, a best designed system was chosen according to the performance analysis results in order for comparing the electrical energy consumption of the building and system production.

An economic evaluation of the selected design was performed by a simplistic approach. Simple payback period of the system was determined in order to decide whether the system is profitable or not. PV module, installation and Balance of the System components prices were determined by taking the PV and BoS prices trends into account.

Consequently, this thesis aims to provide a reference point for possible and similar future works and try to fill a gap in this field as a limited number of studies were conducted with respect to the photovoltaic system designs in northern countries.

10. Resümee

Käesolev töö keskendub Tallinna Tehnikaülikooli Spordihoone katusele sobiva *on-grid* päikesepaneelide süsteemi tehnilisele lahendusele, sisaldades informatsiooni hoone geograafilise asukoha ja eripäraga seotud parameetrite ja PV-moodulite paiknemise kohta, samuti PV-moodulite ja inverterite valikut, päikesepaneelide reastuse ja paiknemise muutusi vastavalt erinevate inverterite nõudmistele, erinevate suurustega kaablite kasutamise võimalusi, varjustuse analüüsi ning erinevaid võimalikke stsenaariume seoses erinevate omavahel sobitatud tehnoloogiate ja PV-moodulite erinevate kaldenurkade kasutamisega.

Töö tuleks arvestada eeluurimusena *on-grid* süsteemi tehnilise lahenduse kohta, kuna see keskendub põhiliselt süsteemi elektrilistele omadustele; lisaks sellele on arvutustele toetudes tehtud mõningaid oletusi, nt. kasutatavate kaablite umbkaudsete pikkuste kohta jne.

Abistava vahendina uurimuse tegemisel on kasutatud PVsyst tarkvaraprogrammi, mis on oma rikkalike funktsioonide ja kõrge keerukusastme tõttu väga laialt tarvitatav. Seda kasutavad arhitektid, teadlased, insenerid ja PV-spetsialistid üle maailma. Suurem osa analüüse selles töös ongi tehtud PVsyst'i abiga. Simulatsioonid on viidud läbi, arvestades erinevate võimalike lahendustena erinevate PV-moodulite, inverterite ja kaldenurkade kasutust, et teha järeldusi neist valikutest lähtuvate erineva tootlikkuse ja efektiivsuse ning süsteemi toimimise võimaluste kohta ja toodetava energia hulga kohta aastas.

On antud ka majandusliku kasumlikkuse hinnang väljavalitud tehnilisele lahendusele, võttes arvesse turuhindu ja vastavaid trende.

Viimaks, kuna vastavasisulisi uurimusi on siiani kirjutatud vaid piiratud hulgal, loodab autor, et käesolev töö võiks olla lähtepunktiks paljudele tulevastele töödele, mis annaksid meile juurde teadmisi päikesepaneelide kasutusvõimalustest põhjamaades.

References

[1]   **European Commission.** *A Proposal for Directive of the European Parliament and of the Council.* Brussels : European Commission, 2012

[2]   **John Duffie, William Beckman.** *Solar Engineering of Thermal Processes.* John Wiley&Sons,Inc. 1980. (p10-13-77)

[3]   **C. Julian Chen**. *Physics of Solar Energy*. John Wiley&Sons, Inc. 2011. (p.1)

[4]   **U.S. Energy Information Administration**. *International Energy Outlook 2013* (IEO2013).2013.(p.1)

[5]   **Heinrich Häberlin**. *Photovoltaics: System Design and Practice*. John Wiley & Sons, Ltd. 2012. (p.27,28-30,13-14,133)

[6]   **Soteris A. Kalogrou**. *Solar Energy Engineering: Processes and Systems*. Elsevier Inc. 2009.(p.55,489)

[7]   **Roger A. Messenger, Jerry Ventre**. *Photovoltaic Systems Engineering*. CRC Press LLC. 2nd edition. 2004. (p.29-23)

[8]   **Newport Corporation**. *Introduction to Solar Radiation*. http://www.newport.com/Introduction-to-Solar-Radiation/411919/1033/content.aspx (09.05.2014)

[9]   **Christiana Honsberg**, **Stuart Bowden.** http://www.pveducation.org (09.05.2014)

[10]   **S.R. Wenham, M.A. Green, M.E. Watt, R. Corkish** *Applied Photovoltaics* 2nd edition. Earthscan. 2007.(p.5)

[11]   **G. N. Tiwari, Swapnil Dubey**. *Fundamentals of Photovoltaic Modules and Their Applications*. RSC Publishing. 2010. (p.23)

[12]   *RETScreen International Photovoltaic Project Analysis Textbook*.(p.22) (Available at: www.retscreen.net)

[13]   http://www.yourhome.gov.au/energy/photovoltaic-systems (23.05.2014)

[14]   **Alternative Energy Tutorials**. *Solar Cell I-V Characteristic and Solar Cell I-V Curve* http://www.alternative-energy-tutorials.com/energy-articles/solar-cell-i-v-characteristic.html (20.05.2014)

[15]   *Battery and Energy Technologies* http://www.mpoweruk.com/solar_power.htm (15.05.2014)

[16]   **Swapnil Dubey, Jatin Narotam Sarvaiya, Bharath Seshadri**. *Temperature Dependent Photovoltaic (PV) Efficiency and Its Effect on PV Production in the World-A Review.* Energy Procedia 33 (2013) 311 – 321. Elsevier. 2013. (p.319)

[17]   **The German Energy Society**. *Planning and Installing Photovoltaic Systems: A guide for installers, architects and engineers 2nd edition* Earthscan. 2008. (p.104,134,91,159)

[18]   **H. Haeberlin**. *Evolution of Inverters for Grid connected PV-Systems from 1989 to 2000* (available at: http://www.pvtest.ch/fileadmin/user_upload/lab1/pv/wr01.pdf)

[19]   http://www.pvsyst.com/ (13.05.2014)

[20]   **University of Geneva**. *PVsyst Contextual Help, 1994-2013.* Available on the website: http://www.pvsyst.com/

[21]   http://www.weatherbase.com/weather/ weatherall.php3?s=83062&cityname=Tallinn%2C+Estonia&units= (16.05.2014)

[22]   **Antonio Luque, Steven Hegedus**. *Handbook of Photovoltaiv Science and Engineering*. John Wiley & Sons 2003 (p.942)

[23]   http://www.pvstudent.com/Inter-row-spacing-calculators.html (16.05.2014)

[24]   **Evo Energy**. *Design Guide* http://www.solarenergysystemsltd.com/images/guide%202.pdf (10.05.2014)

[25]   **André Mermoud** *Shading mismatch loss calculation in PVsyst 6.* Sandia National Laboratories 2013 available at: http://energy.sandia.gov/wp/wp-content/gallery/uploads/31-Mermoud ShadingMismatchLoss_Sandia_May13.pdf0_.pdf

[26]   **David L. King, Jay A. Kratochvil** *Temperature Coefficients For PV Modules and Arrays: Measurement Methods, Difficulties and Results*

[27]   **Didier Thevenard** *Uncertainty in Long-Term Photovoltaic Yield Predictions* Canmet ENERGY 2010 (p.19)

[28]   **Chetan Singh Solanki** *Solar Photovoltaic Technology and Systems: A Manual for Technicians, Trainers and Engineers* PHI Learning Private Limited, Delhi. 2013 (p.268)

[29] **International Electrotechnical Commission** *IEC 61724 Photovoltaic System Performance Monitoring – Guidelines for Measurement, Data Exchange and Analysis* Geneva, 1998

[30] **B. Marion, J. Adelstein, and K. Boyle** *Performance Parameters for Grid-Connected PV Systems* National Renewable Energy Laboratory 2005

[31] **Betterbricks**. *High Performance Portfolio: Rethinking Simple Payback Period* Available at: http://www.betterbricks.com/graphics/assets/documents/ReThinking_Simple_Payback _9.09.pdf (22.05.2014)

[32] **F. John Hay**. *Economics of Solar Photovoltaics* University of Nebraska-Lincoln and the United States Department of Agriculture. 2013 Available at: http://www.ianrpubs.unl.edu/live/g2182/build/g2182.pdf

[33] **International Renewable Energy Agency** *Renewable Energy Technologies: Cost Analysis SeriesVolume 1: Power Sector Issue 4/5*. 2012 Available at: http://www.irena.org/DocumentDownloads/Publications/RE_Technologies_Cost_Ana lysis-SOLAR_PV.pdf

[34] **Elering**. http://elering.ee/renewable-energy-subsidy-2/ (12.05.2014)

[35] **Rünno Lumiste.** *How Expensive Is It to Support Renewable Energy in Estonia?* Baltic Journal of European Studies. Tallinn University of Technology (ISSN 2228-0588), Vol. 2, No. 1 (11)

[36] **SharpND-R250A5/TechnicalDataSheet**
http://www.belectric.com/fileadmin/MASTER/pdf/datasheet/111108%20Sharp_Fly er_ND_Serie_60_A5_0811_EN.pdf (04.26.2014)

[37] **SharpNU-R250J5///TechnicalDataSheet**
http://www.rexelrenewableenergy.co.uk/FileDepository/TechDocs/Modules/Sharp% 20245%20Module%20Datasheet.pdf (26.04.2014)

[38] **HuaweiTech.SUN2000-28k///TechnicalDataSheet**
http://www.google.ee/url?sa=t&rct=j&q=&esrc=s&source=web&cd=2&ved=0CC0Q FjAB&url=http%3A%2F%2Fenterprise.huawei.com%2Filink%2Fcnenterprise%2Fdo wnload%2FHW_274403&ei=ORWOU7CqFuTZ4QTfroGwAw&usg=AFQjCNFaTX m2w32W0IvrDXOHTBKGa8xdmw&sig2=Tu8LuWcyxOFvfm3OiooY0w&bvm=bv. 68191837,d.bGE (28.04.2014)

[39] **SamilPowerSolarLake25000TL-PM///TechnicalDataSheet**
http://www.enfsolar.com/ApolloF/solar/Product/pdf/Inverter/52089cbd55eb3.pdf (05.05.2014)

[40] **PLATINUM13000TLD///TechnicalDataSheet**   http://www.platinum-nes.com/product/solar-inverter/three-phase-solar-inverter/tld-serie-13-to-22-kw/ (05.05.2014)

Appendices

APPENDIX 1

Figure A1-1: Sharp ND-R250A5 (Polycrystalline) /page1 [36]

ELECTRICAL DATA (AT STC)

		ND-R250A5	ND-R245A5	ND-R240A5	ND-R235A5	ND-R230A5	
Maximum power	P_{max}	250	245	240	235	230	W_p
Open-circuit voltage	V_{OC}	37.6	37.3	37.2	36.8	36.4	V
Short-circuit current	I_{SC}	8.68	8.62	8.57	8.49	8.41	A
Voltage at point of maximum power	V_{mpp}	30.9	30.7	30.4	30.3	30.3	V
Current at point of maximum power	I_{mpp}	8.10	7.99	7.90	7.76	7.61	A
Module efficiency	η_m	15.2	14.9	14.6	14.3	14.0	%

STC = Standard Test Conditions: irradiance 1,000 W/m², AM 1.5, cell temperature 25 °C.
Rated electrical characteristics are within ±10% of the indicated values of I_{SC}, V_{OC} and 0 to +5% of P_{max} (power measurement tolerance ±3%).

ELECTRICAL DATA (AT NOCT)

		ND-R250A5	ND-R245A5	ND-R240A5	ND-R235A5	ND-R230A5	
Maximum power	P_{max}	180.2	176.6	173.0	169.3	165.7	W_p
Open-circuit voltage	V_{OC}	36.7	36.4	36.4	36.0	35.6	V
Short-circuit current	I_{SC}	7.0	6.96	6.92	6.85	6.79	A
Voltage at point of maximum power	V_{mpp}	27.7	27.5	27.2	27.1	27.1	V
Nominal Operating Cell Temperature	NOCT	47.5	47.5	47.5	47.5	47.5	°C

NOCT: Module operating temperature at 800 W/m² irradiance, air temperature of 20 °C, wind speed of 1 m/s.

LIMIT VALUES

|	
Maximum system voltage	1,000 V DC
Over-current protection	15 A
Temperature range	−40 bis +90 °C
Maximum mechanical load	2,400 N/m²

MECHANICAL DATA

Length	1,652 mm (+/−3.0 mm)
Width	994 mm (+/−2.0 mm)
Depth	46 mm (+/−0.8 mm)
Weight	19 kg

TEMPERATURE COEFFICIENT

P_{max}	−0.440 % / °C
V_{OC}	−0.329 % / °C
I_{SC}	+0.038 % / °C

CHARACTERISTIC CURVES ND-R250A5

Characteristic curves: current / power vs. voltage (cell temperature: 25 °C)
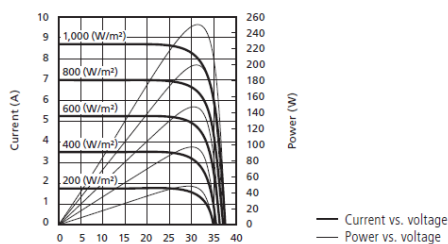
REAR VIEW
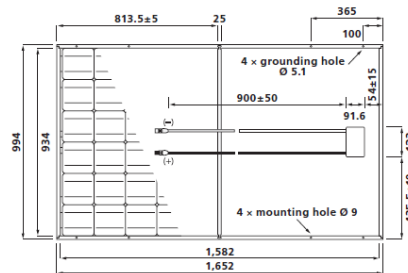
GENERAL DATA

Cells	polycrystalline, 156.5 mm × 156.5 mm, 60 cells in series
Front glass	low iron tempered glass, 3 mm
Frame	anodized aluminium alloy, silver
Connection box	PPE/PPO resin, IP65 rating, 58 × 125 × 15 mm, 3 bypass diodes
Cable	4 mm², length 900 mm
Connector	SMK (MC4 compatible), Type CCT9901-2361F/2451F (Catalogue no. P51-7H/R51-7), IP67 rating. To extend the module connection leads, only use SMK connector from the same series or MultiContactAG MC4 connector (PV-KST04/PV-KBT04)

REGISTRATION

Sharp Solar guarantees the safety, quality and value of your product over many years – the only thing we ask you to do is to register your modules with the serial number, so that we can send you the guarantee certificate. Register your modules quickly and easily at **www.brandaddedvalue.net.**

Sharp Energy Solution Europe · a division of Sharp Electronics (Europe) GmbH · Sonninstrasse 3, 20097 Hamburg, Germany · Tel: +49(0)40/2376-0 · Fax: +49(0)40/2376-2193

www.sharp.eu/solar

SHARP

Local responsibility:
Austria SolarInfo.at@sharp.eu
Benelux SolarInfo.seb@sharp.eu
Central & Eastern Europe SolarInfo.scee@sharp.eu
Denmark SolarInfo.dk@sharp.eu
France SolarInfo.fr@sharp.eu
Germany SolarInfo.de@sharp.eu
Scandinavia SolarInfo.sen@sharp.eu
Spain & Portugal SolarInfo.es@sharp.eu
Switzerland SolarInfo.ch@sharp.eu
United Kingdom SolarInfo.uk@sharp.eu

SunFields Europe · Lope Gomez de Marzoa, Feuga 12, 15706, Santiago de Compostela, Spain · Tel: +34 981595856 · Email: info@sfe-solar.com

Figure A1-2: Sharp ND-R250A5 (Polycrystalline) /page2 [36]

SHARP

Say yes to solar power!
Because it protects the climate.

Innovations from a photovoltaic pioneer

As a solar specialist with more than 50 years of experience in photovoltaics (PV), Sharp makes significant contributions to groundbreaking progress in solar technology.

Sharp photovoltaic modules in the NU series are designed for applications with high power requirements. These quality monocrystalline modules produce a continuous, reliable yield, even under demanding operational conditions.

All Sharp NU series modules offer system integration which is optimal both technically and economically, and are suitable for installations in on and off-grid PV systems.

Certificates and approvals

All modules are tested and certified according to
- IEC/EN 61215 and IEC/EN 61730, Application class A
- Safety class II
- CE

Sharp is certified based on
- ISO 9001:2008 and ISO 14001:2004

Product features

- High-performance photovoltaic modules made of monocrystalline (156.5 mm)² silicon solar cells with module efficiencies of up to 15.2%.
- Anti-reflex coating to increase light absorption.
- Production controlled positive power tolerance from 0 to +5%. Only modules will be delivered that have the specified power or more for high energy yield.
- Delivery of modules in 5-watt intervals.
- Improved temperature coefficient to reduce power losses at higher temperatures.
- High power performance even at lower irradiations.

Quality from Sharp

Benchmarks are set by the quality standards of Sharp Solar. Continual checks guarantee a consistently high level of quality. Every module undergoes visual, mechanical, and electrical inspection. This is recognisable by means of the original Sharp label, the serial number, and the Sharp guarantee:

- 5-year product guarantee
- 10-year performance guarantee on a power output of 90%
- 25-year performance guarantee on a power output of 80%

The detailed guarantee conditions and additional information can be found at **www.sharp.eu/solar.**

As at: June 2011

Figure A1-3: Sharp NU-R250J5 (Mono-crystalline) /page1[37]

Electrical data (at STC)

		NU-R250J5	NU-R245J5	NU-R240J5	
Maximum power	P_{max}	250	245	240	W_p
Open-circuit voltage	V_{OC}	37.9	37.5	37.3	V
Short-circuit current	I_{SC}	8.76	8.73	8.63	A
Voltage at point of maximum power	V_{mpp}	31.0	30.5	30.2	V
Current at point of maximum power	I_{mpp}	8.07	8.04	7.95	A
Module efficiency	η_m	15.2	14.9	14.6	%

STC = Standard Test Conditions: irradiance 1,000 W/m², AM 1.5, cell temperature 25°C.
Rated electrical characteristics are within ±10% of the indicated values of I_{SC}, V_{OC} and 0 to +5% of P_{max} (power measurement tolerance ±3%).

Electrical data (at NOCT)

		NU-R250J5	NU-R245J5	NU-R240J5	
Maximum power	P_{max}	179.9	176.3	172.7	W_p
Open-circuit voltage	V_{OC}	37.1	36.7	36.5	V
Short-circuit current	I_{SC}	7.07	7.05	6.96	A
Voltage at point of maximum power	V_{mpp}	27.9	27.4	27.1	V
Nominal Operating Cell Temperature	NOCT	47.5	47.5	47.5	°C

NOCT: Module operating temperature at 800 W/m² irradiance, air temperature of 20°C, wind speed of 1 m/s.

Limit values

Maximum system voltage	1,000 V DC
Over-current protection	15 A
Temperature range	−40 to +90 °C
Maximum mechanical load	2,400 N/m²

Mechanical data

Length	1,652 mm (+/−3.0 mm)
Width	994 mm (+/−2.0 mm)
Depth	46 mm (+/−0.8 mm)
Weight	19 kg

Temperature coefficient

P_{max}	−0.463 % / °C
V_{OC}	−0.330 % / °C
I_{SC}	+0.030 % / °C

Characteristic curves NU-R245J5

Characteristic curves: current / power vs. voltage (cell temperature: 25°C)

Rear view
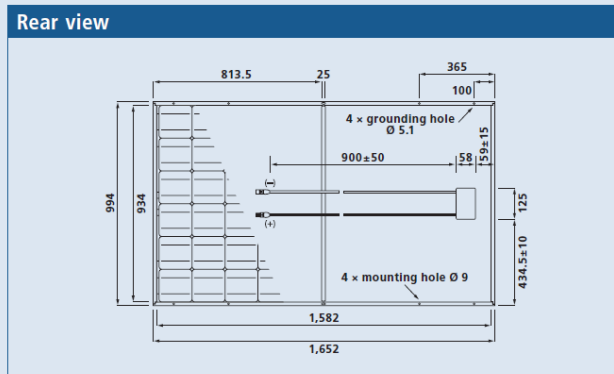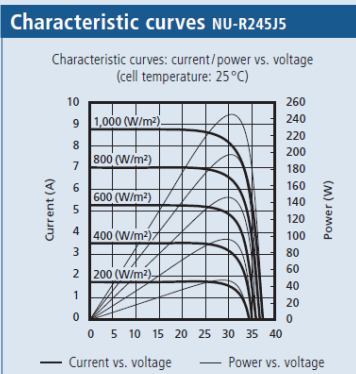
General data

Cells	monocrystalline, 156.5 mm × 156.5 mm, 60 cells in series
Front glass	low iron tempered glass, 3 mm
Frame	anodized aluminium alloy, silver
Connection box	PPE/PPO resin, IP65 rating, 58 × 125 × 15 mm, 3 bypass diodes
Cable	4 mm², length 900 mm
Connector	SMK (MC4 compatible), Type CCT9901-2361F/2451F (Catalogue no. P51-7H/R51-7), IP67 rating

To extend the module connection leads, only use SMK connector from the same series or MultiContactAG MC4 connector (PV-KST04/PV-KBT04)

Registration

Sharp Solar guarantees the safety, quality and value of your product over many years – the only thing we ask you to do is to register your modules with the serial number, so that we can send you the guarantee certificate. Register your modules quickly and easily at **www.brandaddedvalue.net.**

Figure A1-4: Sharp NU-R250J5 (Mono-crystalline) /page2 [37]

SUN2000 Series -28KTL

SUN2000-28KTL

The maximum efficiency of SUN2000-28KTL is up to 98.7% with "T" type three level topology. It supports 3 MPPT for versatile adaption to different module types or quantities built up with different alignments. It adopts natural cooling technology without external fan to increase reliability and save maintenance. The output voltage is 480V, which reduces AC cable power loss up to 30%. SUN2000-28KTL string inverter is the best solution for large scale PV plant.

SUN2000-28KTL meets Germany BDEW MV directive and VDE1206-1-1 directive, CE Low Voltage Directive and the Directive for Electromagnetic Compatibility, as well as China Golden Sun certification. It has good environment adaptability especially for the large scale medium voltage PV plant with IP65 and fanless design.

7

Figure A1-5: Huawei Tech. SUN2000-28k/page1 [38]

Higher Yields

- Maximum efficiency 98.7%
- European efficiency 98.4%
- Reduce 30% AC cable loss with higher output voltage of 480V
- Saving AC cable investment up to 20% without N-Line

High Reliability

- With 20 years technology accumulation in telecom power, the same platform building inverter product
- No need of external fan with natural cooling technology
- Type II DC and Type III AC surge protection devices integrated
- Warranty up to 25 years

Smart

- Maximum of 3 MPPT for versatile adaption to different module types or quantities built up with different alignments
- Up to 6 strings intelligent monitoring and fault detection
- Local graphic LCD and remote monitoring
- RS 485 and USB ports for connectivity and data management

Friendly

- 48kg@27.5kW, compact design of 0.08m³
- Easy connection with external waterproof DC / AC and signal terminals
- Noise ≤ 29dB
- Outdoor application of IP65

Efficiency Curve

Circuit Diagram

8
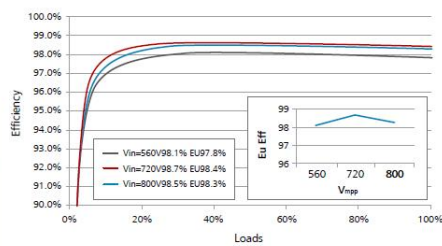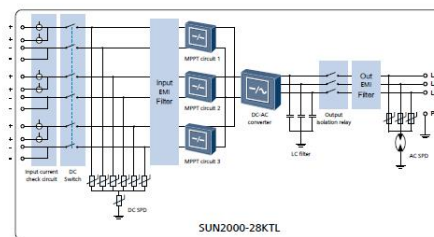
Figure A1-6: Huawei Tech. SUN2000-28k/page2 [38]

Technical Specifications

| Technical Specifications		SUN2000-28KTL	
Efficiency		**Protection**	
Max. efficiency	98.7%	Input-side disconnection device	Yes
European efficiency	98.4%	Anti-Islanding protection	Yes
Input		AC over current protection	Yes
Max. DC input (cos φ =1)	28,200 W	DC reverse-polarity protection	Yes
Max. input voltage	1000 V	PV-array string fault monitoring	Yes
Max. input current	18 A	DC surge arresters	Type II
Min. operating voltage	200 V	AC surge arresters	Type III
MPP voltage range	480 V~800 V	Insulation monitoring	Yes
Rated input voltage	620 V	Residual current detection	Yes
Max. number of inputs	6	**General Data**	
Number of MPP trackers	3	Dimensions(W/H/D)	520x610x255 mm (20.5 x 24.0 x 10.0 in.)
Output		Weight	48 kg
Rated power	27,500 W	Operating temperature range	-25°C to +60°C (-13°F to +140°F)
Rated output voltage	3 × 277 V/480 V+PE	Cooling	Natural convection
AC power frequency	50 Hz/60 Hz	Operating altitude	3000 m
Max. output current	33.5 A	Relative humidity (non-condensing)	0~100%
Adjustable power factor	0.8 leading ... 0.8 lagging	DC connector	Amphenol H4
Max. total harmonic distortion	<3%	AC connector	Amphenol C16/3
Display and Communication		Degree of protection	IP65
Display	Graphic LCD	Self-consumption at night	< 1 W
RS485	Yes	Topology	Transformerless
USB	Yes	Noise emission	29dB
		Warranty	5 years (10/15/20/25 years optional)
Standards Compliance			
Safety/EMC	EN61000-6-2, EN61000-6-3, EN61000-3-2, EN61000-3-3, EN61000-3-11, EN61000-3-12, EN/IEC62109-1, EN/IEC62109-2		
Grid code	VDE0126-1-1, BDEW 2008, CGC/GF004: 2011		

9

Figure A1-7: Huawei Tech. SUN2000-28k/page3 [38]

PV Grid-tied Inverter (Three phase)

SolarLake 25000TL-PM/30000TL-PM

LEADING-EDGE TECHNOLOGY
- Flexible PV system design due to the extensive input voltage range
- Maximum power yield under different orientation or partial shade due to two independent MPP trackers
- Integrated self-consumption control and environmental data logger
- Power reduction and reactive power control
- Optional equipped with earth fault alarm system (for AU market)
- Array combiner function optional with DC switch/AC switch/fuse/surge protection/current & voltage measurement for all strings
- Transformerless - minimizing size and weight
- Maximum efficiency 98%

FLEXIBILITY
- Use for indoor and outdoor (IP65)
- Fast installation and reduction transportation costs due to lighter weight aluminum housing
- "Plug and Play" connection for easy installation and maintenance
- Multi-lingual display
- Easy configuration for different country grid standards

BUILT TO LAST
- Automatic protection against over/under voltage, over/under load, islanding, short circuit
- 5 years standard warranty, up to 25 years warranty extension

CERTIFICATES
- CE, TUV, VDE 0126-1-1, RD 1669, G59, DK5940, EN50178, EN61000-3-2, EN6100-6-1/2/3/4, IEC-62109, VDE AR-N-4105, BDEW, CEI 0-21, CEI 0-16, AS4777, CQC (6-10, 25-30)

SAMIL POWER
Expert for PV Grid-tied Inverters

Figure A1-8: Samil Power Solar Lake 25000TL-PM /page1 [39]

Datasheet of SolarLake Series

Inverter model	SolarLake 25000TL-PM	SolarLake 30000TL-PM
Input (DC)		
Max. DC power [W]	27600	32000
Max. DC voltage [V]	1000	
Max. input current [A]	A: 35/B:35	
Feed-in start voltage [V]	350	
Operating voltage range [V]	250-950	
MPPT voltage range (full load) [V]	460-850	
Numbers of MPPT	2	
Strings per MPPT	1/4 (optional)	
DC switch	Optional	
Output (AC)		
Rated AC power [W]	25000	30000
Max. AC power [W]	25000	30000
Max. AC current [A]	35.5	43.5
Rated AC voltage/range [V]	3/N/PE, 230/400	
Rated AC frequency/range [Hz]	45-55Hz/54-66Hz	
Power factor (cos ϕ)	0.8 lagging-0.8 leading	
THDi (at rated power)	<3%	
Efficiency		
Max. efficiency	98.2%	
Euro efficiency	98.0%	
MPPT efficiency	99.9%	
General Data		
Dimensions (WxHxD) [mm/in]	600x880x239/23.6x34.6x9.4	
Weight [kg/lb]	60/132	
Operating temperature range [°C/°F]	-25-+60/-13-140	
Cooling	Fan	
Ingress protection (IP)	IP65	
Display	3.5 inch LCD	
Communication	Ethernet (standard)/Goldfinger (standard)/RS485 (standard)/Wi-Fi (standard)/Zigbee (optional)	
Warranty (5/10/15/20/25 years)	standard/optional/optional/optional/optional	
Certificates	CE, TUV, BDEW, CEI 0-16, VDE 0126-1-1, RD 1669, G59, DK5940, EN50178, EN61000-3-2, EN6100-6-1/2/3/4, IEC-62109, VDE AR-N-4105, CEI 0-21, AS4777, CQC (6-10, 25-30)	

V-001 EN
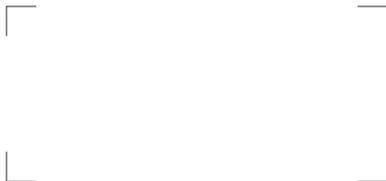
www.samilpower.com

Figure A1-9: Samil Power Solar Lake 25000TL-PM /page2 [39]

Delivering an impressive efficiency of 98 %.
The three-phase PLATINUM® TL inverter.
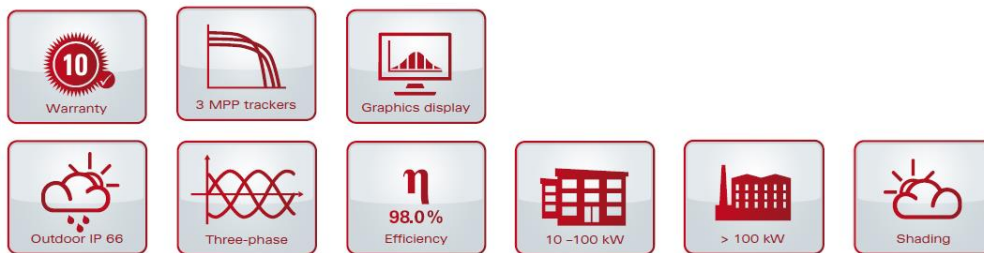
All PLATINUM® TL models are compliant with the "Energy Management (§6 EEG)" market requirement specification, the "Technical Guidelines for Power Generating Plants Connected to the Medium Voltage Grid" and the "Low-voltage Directive AR-N-4105" as of its coming into effect as the successor directive of VDE 0126-1-1.

Figure A1-10: PLATINUM 13000 TLD /page1 [40]

Specifications

TL inverter	13000 TL	16000 TL	19000 TL
DC Input			
Max. PV power	14,700 Wp	18,000 Wp	21,300 Wp
Max. DC power (@ cos phi = 1)	12,900 W	15,900 W	18,900 W
MPPT voltage range	351 ... 710 V	349 ... 710 V	350 ... 710 V
Max. input voltage	880 V		
Max. MPPT inout current	3 x 13 A	3 x 16 A	3 x 18.5 A
Number of string inputs	6		9
Number of MPP trackers	3		
DC disconnector	○		
DC short circuit current	3 x 18 A	3 x 22 A	3 x 26 A
Reverse polarity protection / Ground fault monitoring (isolation check)	● / ●		
AC Output			
Rated power (@ cos phi = 1)	12,360 W	15,000 W	18,000 W
Rated current	3 x 17.9 A	3 x 21.7 A	3 x 26.1 A
Max. apparent power	12,360 VA	15,000 VA	18,000 VA
Max. AC current	3 x 17.9 A	3 x 21.7 A	3 x 26.1 A
Power feed starts at	21 W		24 W
Mains output voltage	3AC 230 V / 400 V (+/-20 %)		
Feed in phases / connection phases	3 / 3		
Max. permitted grid impedance [Zmax] (EN 61000-3-11)	424 mΩ	349 mΩ	290 mΩ
Standby consumption	3 W		
Mains frequency	50 Hz (+/-5 %)		
Power factor (cos phi) (ind ... kap)	0.7 ... 0.7		
Short circuit resistance / Ground fault monitoring (RCD)	● / ●		
Interfaces			
DC connection	MC4		
AC connection	Spring clamp connectors		
RS 485 (Clamps / RJ45)	● / ●		
Ethernet / CAN	– / –		
Integrated web server	–		
Alarm relay	24 V_{AC} / 2 A		
Appliance data			
Max. efficiency	97.7 %		97.9 %
European efficiency	97.4 %		97.5 %
Weight	81 kg	84 kg	87 kg
Dimensions (H x W x D in mm)	743 x 972 x 262		
Operating temperature	-20 ... +60 °C		
Storage temperature	-25 ... +80 °C		
Relative humidity	0 ... 95 %		
Altitude at rated power	2,000 m / 6,560 ft		
Protection degree (except digital interface)	IP 65		
Protection class / overvoltage category	I / Type 3		
Full graphic display (color / monochrome)	– / ●		
Storage capacity data logger	30 years		
System topology	Transformerless		
Cooling	Convection	Fan	
Standards / grid codes	VDE 0126-1-1, VDE AR-N 4105, BDEW 2008, CEI 0-21, C10/11, G83/2, G59/2, EN 50438, ÖNORM E8001-4-712, UTE C15-712-1, RD 1699/661, IEC 62109, AS 4777, AS 3100		
Warranty	10 years		
Type designation	**13000 TLD**	**16000 TLD**	**19000 TLD**

Subject to alterations. Valid as of 04/2013. More than 45 countries are currently supported. The current list is available from the download area of our homepage www.platinum-nes.com

● Standard   ○ Optional   – Not available

Figure A1-11: PLATINUM 13000 TLD /page2 [40]

APPENDIX 2

SUMMARY OF THE WORLDWIDE MARKET PRICE OF PV MODULES , Q4 2009 to Q1 2012

Factory-gate price in Europe (USD/Watt)

PV module suppliers	2009 Q4	2010 Q1	Q2	Q3	Q4	2011 Q1	Q2	Q3	Q4	2012 Q1
High efficiency c-Si	2.45	2.22	2.25	2.29	2.21	2.20	2.15	2.10	2.00	1.94
Japanese/Western c-Si **	1.98	1.81	1.83	1.74	1.66	1.40	1.27	1.08	1.22	1.22
Chinese major c-Si ***	1.51	1.42	1.52	1.51	1.45	1.39	1.39	1.39	1.39	1.24
Emerging economies c-Si ****	1.45	1.35	1.42	1.43	1.43	1.36	1.31	1.03	1.02	1.02
High efficiency thin-film (via distribution, First Solar)	1.26	1.30	1.39	1.37	1.27	1.16	1.05	0.98	0.93	0.93

Factory-gate price in the United States (USD/Watt)

	2009 Q4	2010 Q1	Q2	Q3	Q4	2011 Q1	Q2	Q3	Q4	2012 Q1
High efficiency c-Si	2.86	2.20	2.55	2.55	2.53	2.30	2.30	2.30	2.30	2.20
Japanese/Western c-Si	2.10	2.05	1.95	1.95	1.93	1.91	1.91	1.91	1.91	1.82
Chinese major c-Si	1.91	1.87	1.83	1.87	1.80	1.43	1.43	1.47	1.43	1.34
Emerging economies- c-Si	1.89	1.75	1.70	1.78	1.74	1.50	1.50	1.50	1.50	1.41
High efficiency thin-film (via distribution, First Solar)	1.21	1.20	1.22	1.25	1.19	1.20	1.22	1.25	0.93	0.93

*Notes: Based on short-term contract prices for quantities of 0.5 MW or more. Spot market prices are typically more volatile. * Sunpower and Sanyo ** Sharp, Kyocera, Solarworld and Schoth *** Suntech, Yungli, Trina Solar and Green Energy, etc. **** Chinese, Korean and Indian manufacturers.*

Table A2-1: Module prices in Europe and in the US [33]

CRYSTALLINE SILICON PV MODULE PRICES PROJECTIONS FOR EUROPEAN, NORTH AMERICAN AND JAPANESE MANUFACTURERS, 2010 TO 2015

High-cost producers	2010	2011	2012	2013	2014	2015
Production scale (MW)	150	400	650	900	1 150	1 400
Polysilicon production (USD/W)	0.43	0.33	0.23	0.18	0.15	0.13
Silicon wafer production (USD/W)	0.46	0.37	0.33	0.29	0.27	0.25
Solar cell production (USD/W)	0.36	0.29	0.25	0.23	0.20	0.19
PV module production (USD/W)	0.50	0.42	0.37	0.33	0.31	0.29
Total PV module cost (USD/W)	**1.75**	**1.41**	**1.18**	**1.03**	**0.93**	**0.85**

Note: Production scale refers to the annual production capacity of a single manufacturing plant required to achieve the cost presented.

Table A2-2: Module price projection table [33]

APPENDIX 3

TALLINN, ESTONIA

Home > Europe > Estonia

Elevation: 43 meters   Latitude: 59 21N   Longitude: 024 48E

Highest Recorded Temperature   Years on Record: 30

	ANNUAL	JAN	FEB	MAR	APR	MAY	JUN	JUL	AUG	SEP	OCT	NOV	DEC
C	34.3	8.9	10.2	15.6	27.2	28.6	30.7	34.3	34.2	28	21.8	12.1	9.4

Lowest Recorded Temperature   Years on Record: 30

	ANNUAL	JAN	FEB	MAR	APR	MAY	JUN	JUL	AUG	SEP	OCT	NOV	DEC
C	-32.2	-31.4	-30	-26.2	-12	-5	0.2	4	2.4	-4.7	-10.5	-18.8	-32.2

Table A3-1: Highest and Lowest recorded temperatures at Tallinn [21]